

## Targeting the Src homology 2 (SH2) domain of signal transducer and activator of transcription 6 (STAT6) with cell-permeable, phosphatase-stable phosphopeptide mimics potently inhibits Tyr641 phosphorylation and transcriptional activity

Pijus K Mandal, Pietro Morlacchi, John Morgan Knight, Todd M Link, Gilbert R. Lee, Roza Nurieva, Divyendu Singh, Ankur Dhanik, Lydia E. Kavrakı, David B. Corry, John E. Ladbury, and John S. McMurray

*J. Med. Chem.*, **Just Accepted Manuscript** • DOI: 10.1021/acs.jmedchem.5b01321 • Publication Date (Web): 27 Oct 2015

Downloaded from <http://pubs.acs.org> on October 31, 2015

### Just Accepted

“Just Accepted” manuscripts have been peer-reviewed and accepted for publication. They are posted online prior to technical editing, formatting for publication and author proofing. The American Chemical Society provides “Just Accepted” as a free service to the research community to expedite the dissemination of scientific material as soon as possible after acceptance. “Just Accepted” manuscripts appear in full in PDF format accompanied by an HTML abstract. “Just Accepted” manuscripts have been fully peer reviewed, but should not be considered the official version of record. They are accessible to all readers and citable by the Digital Object Identifier (DOI®). “Just Accepted” is an optional service offered to authors. Therefore, the “Just Accepted” Web site may not include all articles that will be published in the journal. After a manuscript is technically edited and formatted, it will be removed from the “Just Accepted” Web site and published as an ASAP article. Note that technical editing may introduce minor changes to the manuscript text and/or graphics which could affect content, and all legal disclaimers and ethical guidelines that apply to the journal pertain. ACS cannot be held responsible for errors or consequences arising from the use of information contained in these “Just Accepted” manuscripts.

1  
2  
3 **Targeting the Src homology 2 (SH2) domain of signal transducer and activator of**  
4 **transcription 6 (STAT6) with cell-permeable, phosphatase-stable phosphopeptide mimics**  
5  
6 **potently inhibits Tyr641 phosphorylation and transcriptional activity.**  
7  
8  
9

10  
11  
12 Pijus K. Mandal,<sup>1</sup> Pietro Morlacchi,<sup>1</sup> J. Morgan Knight,<sup>1</sup> Todd M. Link,<sup>2</sup> Gilbert R. Lee, IV,<sup>2</sup>  
13  
14 Roza Nurieva,<sup>3</sup> Divyendu Singh,<sup>3</sup> Ankur Dhanik,<sup>4</sup> Lydia Kavraki<sup>4</sup>, David B. Corry,<sup>5</sup> John E.  
15  
16 Ladbury,<sup>2</sup> John S. McMurray<sup>1\*</sup>  
17  
18  
19

20  
21  
22 <sup>1</sup>Department of Experimental Therapeutics, <sup>2</sup>Department of Biochemistry and Molecular  
23  
24 Biology, Center for Biomolecular Structure and Function, <sup>3</sup>Department of Immunology, The  
25  
26 University of Texas M. D. Anderson Cancer Center, Houston, Texas, <sup>4</sup>The Department of  
27  
28 Computer Science, Rice University, Houston, Texas, <sup>5</sup> Departments of Medicine and Pathology  
29  
30 & Immunology, The Baylor College of Medicine, Houston, Texas  
31  
32  
33  
34  
35

36 Current Addresses:

37  
38  
39 John E. Ladbury

40  
41  
42 School of Molecular and Cellular Biology

43  
44  
45 University of Leeds

46  
47  
48 LC Miall Building

49  
50  
51 Leeds, LS2 9JT

52  
53  
54 UK

55  
56  
57 [J.E.Ladbury@leeds.ac.uk](mailto:J.E.Ladbury@leeds.ac.uk)

58  
59  
60 Pietro Morlacchi

1  
2  
3 Institute for Applied Cancer Science  
4  
5 The University of Texas M. D. Anderson Cancer Center  
6  
7 1901 East Road.  
8  
9 Houston, Tx 77054  
10

11  
12  
13 Todd M. Link  
14  
15 Department of Genomic Medicine  
16  
17 The University of Texas M. D. Anderson Cancer Center  
18  
19 1901 East Road.  
20  
21 Houston, Tx 77054  
22  
23  
24  
25  
26  
27  
28  
29  
30  
31  
32  
33  
34  
35  
36  
37  
38  
39  
40  
41  
42  
43  
44  
45  
46  
47  
48  
49  
50  
51  
52  
53  
54  
55  
56  
57  
58  
59  
60

## Abstract

Signal transducer and activator of transcription 6 (STAT6) transmits signals from cytokines IL-4 and IL-13 and is activated in allergic airway disease. We are developing phosphopeptide mimetics targeting the SH2 domain of STAT6 to block recruitment to phosphotyrosine residues on IL-4 or IL-13 receptors and subsequent Tyr641 phosphorylation to inhibit the expression of genes contributing to asthma. Structure-affinity relationship studies showed that phosphopeptides based on Tyr631 from IL-4R $\alpha$  bind with weak affinity to STAT6 whereas replacing the pY+3 residue with simple aryl and alkyl amides resulted in affinities in the mid to low nM range. A set of phosphatase-stable, cell-permeable prodrug analogs inhibited cytokine-stimulated STAT6 phosphorylation in both Beas-2B human airway cells and primary mouse T-lymphocytes at concentrations as low as 100 nM. IL-13-stimulated expression of CCL26 (eotaxin-3) was inhibited in a dose-dependent manner, demonstrating that targeting the SH2 domain blocks both phosphorylation and transcriptional activity of STAT6.

## Introduction

Signal transducer and activator of transcription 6 (STAT6) transmits signals from cytokines interleukin 4 (IL-4) and IL-13.<sup>1-3</sup> Under normal conditions, STAT6 is required for helper T cell type 2 (Th2) development in the context of allergic inflammatory responses and is hypothesized to contribute to the polarization of macrophages to the M2 phenotype.<sup>4</sup> Upon receptor binding, both IL-4 and IL-13 induce phosphorylation of tyrosine residues located within the intracellular region of IL-4R $\alpha$  (Figure 1). STAT6, via its SH2 domain, is recruited to these phosphotyrosine residues and is itself phosphorylated on Tyr641 by associated Janus kinases 1 and 3 (JAK1 and JAK3). Tyrosine phosphorylated STAT6 (pSTAT6) then dimerizes via reciprocal SH2 domain-

pTyr interactions, allowing it to translocate to the nucleus, where it participates in the transcription of allergy-related genes. The IL-4/IL-13/JAK/STAT6 pathway plays a key role in asthma pathogenesis.<sup>1,2</sup> Patients have elevated levels of IL-4 and IL-13 in their airways and elevated pSTAT6 levels have been found in bronchial epithelium.<sup>5</sup> *Stat6* knockout mice do not develop airway hyperresponsiveness (AHR) or lung pathology associated with asthma.<sup>6</sup>

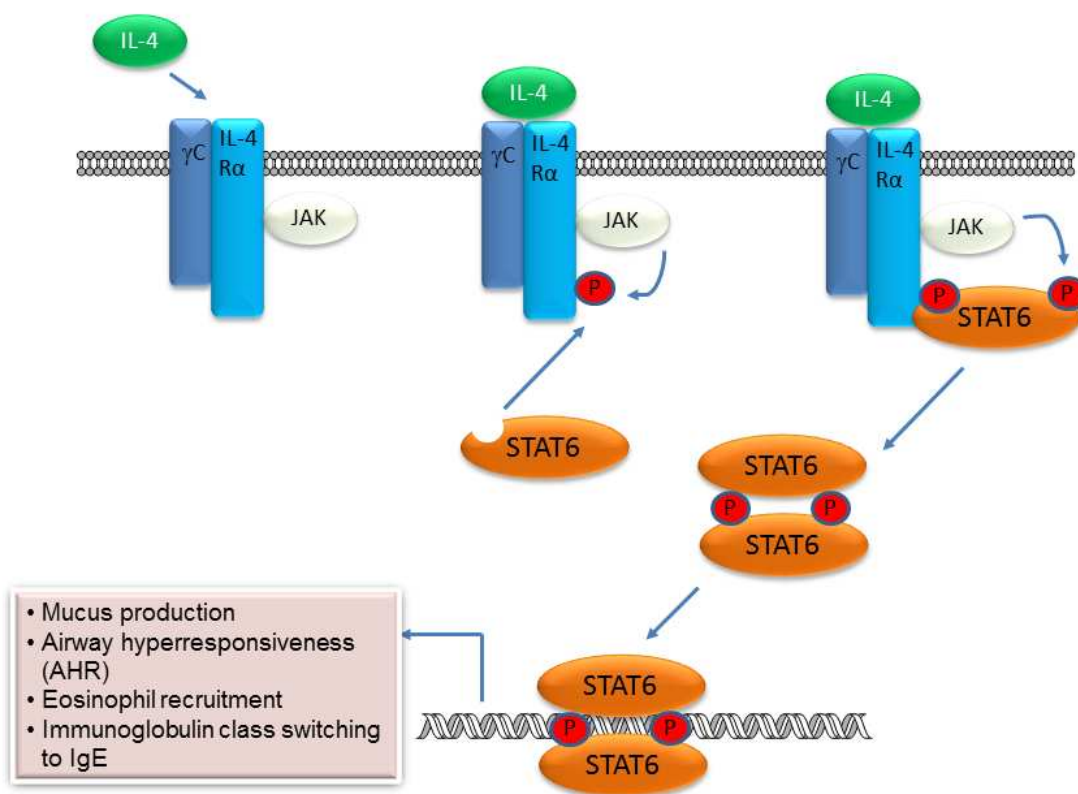


**Figure 1.** Schematic representation of the IL-4/JAK/STAT6 pathway. Note the IL-13 signals in an analogous manner using the IL-13R1/IL-4R $\alpha$  co-receptor.

Intervention in the IL-4/IL-13/JAK/STAT6 pathway at several points for the treatment of asthma is being actively pursued by the pharmaceutical industry and academic laboratories.<sup>1,2</sup> These include small molecules without described inhibitory mechanisms,<sup>7-12</sup> non-SH2 domain

1  
2  
3 directed dimerization inhibitors,<sup>13</sup> JAK inhibitors,<sup>14, 15</sup> siRNA,<sup>6</sup> decoy oligonucleotides,<sup>16</sup>  
4  
5 phosphopeptides targeting the SH2 domain of STAT6,<sup>17-19</sup> antibodies targeting IL-13<sup>20</sup> and  
6  
7 antibodies targeting IL-4R $\alpha$ .<sup>20-22</sup> Our approach is to target the SH2 domain of STAT6 with  
8  
9 small molecule peptidomimetics to block recruitment to IL-4R $\alpha$  thereby preventing subsequent  
10  
11 phosphorylation of Tyr641 by JAKs, dimerization, translocation to the nucleus, and transcription  
12  
13 of genes leading to airway inflammation. Proof of principle that steric blockade of the SH2  
14  
15 domain of STAT6 prevents recruitment to IL-4R $\alpha$ , phosphorylation of Tyr641, and subsequent  
16  
17 transcriptional activity leading to asthma symptoms has been demonstrated using  
18  
19 phosphopeptides derived from Tyr631 of IL-4R $\alpha$ , the docking site for STAT6,<sup>18</sup> and Tyr641 of  
20  
21 STAT6,<sup>17, 19</sup> with cell penetration peptides attached.  
22  
23  
24  
25  
26

27  
28 To the best of our knowledge, no systematic structure-affinity or structure-activity studies  
29  
30 of phosphopeptide ligands of the SH2 domain of STAT6 have appeared in the literature. In this  
31  
32 communication we report truncation and amino acid substitutions on a phosphopeptide based on  
33  
34 the sequence surrounding Tyr631 of IL-4R $\alpha$  to gain an understanding of the determinants for  
35  
36 binding affinity that could be used in the design of STAT6 antagonists. In parallel, a structure-  
37  
38 affinity study of phosphate analogs of a phosphopeptide mimic reported in the patent literature<sup>23</sup>,  
39  
40 <sup>24</sup> was also conducted. A molecular docking study illustrated key intramolecular interactions that  
41  
42 help explain the higher affinity of the mimics compared to the receptor-derived peptide ligand.  
43  
44 Bis-POM prodrugs of phosphatase-stable phosphonodifluoromethyl analogs of a set of the new  
45  
46 inhibitors provided a structure-activity relationship for inhibition of IL-4 and IL-13 stimulated  
47  
48 phosphorylation of Tyr641 in intact human airway epithelial cells. Several inhibitors induced  
49  
50 significant inhibition at 100-500 nM in this cell line as well as in a human breast cancer cell line  
51  
52 and primary murine T lymphocytes. Expression of the downstream target, CCL26 (eotaxin-3)  
53  
54  
55  
56  
57  
58  
59  
60

1  
2  
3 was inhibited, which demonstrates that, in addition to inhibition of Tyr641 phosphorylation, this  
4  
5 class of compounds blocks transcriptional activity of STAT6.  
6  
7

## 8 **Results**

9  
10 **Affinity of phosphopeptides for STAT6.** To understand basic requirements for phosphopeptide  
11  
12 binding to the SH2 domain and to possibly find a lead for peptide mimetic development, we  
13  
14 screened a series of peptides based on the STAT6 docking site of IL-4R $\alpha$ , Tyr 631. As SH2  
15  
16 domains typically recognize phosphotyrosine and two to four residues on its C-terminal side,<sup>25, 26</sup>  
17  
18 we prepared a series of N-terminal pTyr phosphopeptides. The fluorescence polarization assay  
19  
20 of Wu et al.<sup>27</sup> was used to monitor affinity. A construct consisting of an N-terminal His<sub>6</sub> tag, the  
21  
22 coiled-coil domain, the DNA binding domain, the linker domain, and the SH2 domain of STAT6  
23  
24 was cloned, expressed in *E. coli*, and purified by nickel IMAC chromatography for use in these  
25  
26 studies. Overall, the peptides displayed rather weak avidity to STAT6 with IC<sub>50</sub> values ranging  
27  
28 from 2 – 6  $\mu$ M (Table 1). Peptide length was important as affinities decreased from the  
29  
30 octapeptide **1**, (IC<sub>50</sub> = 2  $\mu$ M) to the tetrapeptide **5**, (IC<sub>50</sub> = 6  $\mu$ M). Substitution of alanine for  
31  
32 lysine at position pY+1 resulted in a significant reduction in affinity, whilst other amino acids  
33  
34 such as tertiary leucine (Tle) and norleucine (Nle) were equipotent to lysine (**7-9**, Table 2). Thus  
35  
36 this position requires at the minimum  $\beta$  substitution and the  $\epsilon$ -amino group of lysine does not  
37  
38 provide interaction energy. A small screen of N-terminal hydrophobic appendages showed no  
39  
40 significant effect on affinity (**10-13**, Table 2) and therefore further elaboration of this position  
41  
42 was not pursued. Replacement of pTyr with constrained surrogates 4-phosphoryloxycinnamide  
43  
44 (**14**) and 7-phosphoryloxyindole-2-carboxamide (**15**), which provided notable improvement in  
45  
46 affinity for phosphopeptide inhibitors of STAT3<sup>28</sup> provided no significant increase in binding to  
47  
48 STAT6 in this series of peptides (Table 3). Interestingly, incorporation of 7-  
49  
50 phosphoryloxybenzofuran-2-carboxamide (**16**) led to a substantial decrease in affinity. This  
51  
52  
53  
54  
55  
56  
57  
58  
59  
60

1  
2  
3 suggests that the NH group of the indole may be close to a hydrogen bond acceptor such as a  
4  
5 carbonyl oxygen which would repel the oxygen atom of the benzofuran. In summary,  
6  
7  
8 phosphopeptides based on Tyr631 of the IL-4R $\alpha$  displayed low affinity for STAT6 protein and  
9  
10 were not useful as leads for inhibitor development.  
11

12  
13 In the late 1990's researchers from Tularik, Inc. recognized the potential of inhibition of  
14  
15 STAT6 for the treatment of allergic airway disease and developed phosphopeptide mimics  
16  
17 targeting the SH2 domain.<sup>23,24</sup> Structure-affinity studies were reported, but only one compound  
18  
19 with the potential to inhibit pSTAT6 in intact cells was described in the patents (**17**, Figure 2).  
20  
21  
22 Compound **17** is a phosphopeptide mimic in which phosphotyrosine is replaced by the  
23  
24 conformationally constrained cinnamate unit. Stability to phosphatases was designed by  
25  
26 replacing phosphate with the phosphonodifluoromethyl group.<sup>29</sup> The negatively charged  
27  
28 phosphonate oxygens were blocked with carboxyesterase-labile pivaloyloxymethyl (POM)  
29  
30 groups as a means to permeate cells.<sup>30</sup> Importantly, no biological evaluation was given, either in  
31  
32 the patents or in peer-reviewed literature; therefore it was not known whether this was a viable  
33  
34 approach for the inhibition of STAT6 phosphorylation. Using our convergent methodology for  
35  
36 the synthesis of phosphopeptide mimic prodrugs targeting SH2 domains,<sup>31,32</sup> we improved the  
37  
38 synthesis of **17** and found that it indeed inhibited both IL-4 and IL-13-stimulated  
39  
40 phosphorylation of STAT6 in Beas-2B cells, an immortalized human bronchial epithelial cell  
41  
42 line. Significant inhibition of pSTAT6 was observed at concentrations  $\geq 1 \mu\text{M}$ .<sup>33</sup>  
43  
44  
45  
46  
47  
48  
49  
50  
51  
52  
53  
54  
55  
56  
57  
58  
59  
60

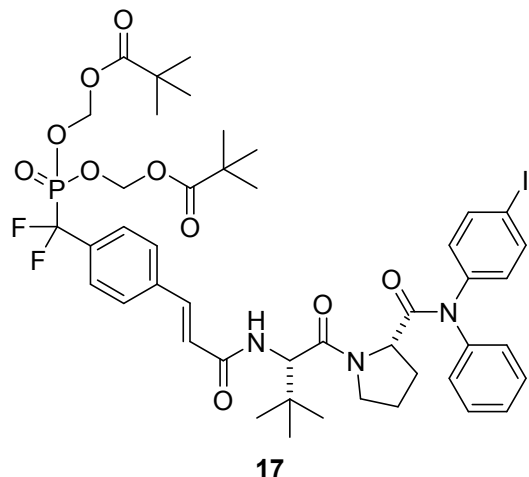


**Figure 2.** Lead STAT6 inhibitor (from reference 33).

We embarked on new studies to test structural requirements of phosphate-containing analogs of prodrug **17** for affinity for the SH2 domain of STAT6. Interestingly, compound **18a** ( $IC_{50} = 0.04 \mu\text{M}$ ) was approximately 100-fold more potent than the phosphopeptides based on the IL-4R $\alpha$  docking site (**1-16**), which exhibited  $IC_{50}$  values of 2-15  $\mu\text{M}$ . Given that **18a** has the cinnamate group of **14** and the Tle-Pro group of **7**, we conclude that placing the aryl groups closer to the proline in **18a** than that of Phe in the peptides is responsible for the increase in affinity. For STAT3 inhibitors, we found that substitution of a methyl group on the  $\beta$  position of the phosphocinnamate pTyr surrogate enhanced affinity 2-3 fold (pCinn vs  $\beta\text{MpCinn}$ ).<sup>31</sup> In keeping with these results, substitution of  $\beta\text{MpCinn}$  for pCinn produced a 2-fold increase in affinity **19a** vs **18a** (Table 4). 7-Phosphoryl-indole 2-carboxylate (**20**) reduced affinity compared to 4-phosphoryloxycinnamate, also consistent with our observations of inhibitors of STAT3.<sup>28</sup>

The literature describing **17** emphasized C-terminal bis-aryl and aryl,benzyl amides and all of the compounds in the reported structure-affinity relationship studies possessed these structural features.<sup>23, 24</sup> To test the requirements of aryl groups, we prepared a series of analogs

1  
2  
3 of **18a** and **19a** with varying C-terminal amide substitution (Table 5). In the cinnamate series,  
4  
5 the diphenylamide (**18b**) has a 3-fold higher IC<sub>50</sub> than **18a** indicating that the iodine contributed  
6  
7 to affinity. Methylanilide **18c** is 4-fold lower in affinity than diphenylamide **18b** suggesting that  
8  
9 aromatics are indeed important at the C-terminus. Removal of the methyl group (**18d**) resulted  
10  
11 in further loss in affinity. Not surprisingly, in the β-methylcinnamate series, the same trend in  
12  
13 affinity loss was observed with reduced aryl and methyl substitution on the C-terminal amide  
14  
15 nitrogen (**19a-d**), although the affinities in this series were higher than those of **18a-d**. No gain  
16  
17 in affinity was achieved by adding one or two methylene unit spacers to anilide **19d**, see **19e** and  
18  
19 **19f**. The cyclohexyl,methyl amide (**19g**) was two-fold less avid than the phenyl,methyl amide,  
20  
21 **19c**. The dimethylamide, **19h**, is significantly lower in affinity than the phenyl,methyl amide.  
22  
23 Affinity is improved with the larger diethylamide, **19i**. These results show that while aryl groups  
24  
25 are important at the C-terminus, reasonable affinity can be achieved with alkyl amides.  
26  
27  
28  
29  
30  
31

32 Structural requirements of proline were probed (Table 6). For these experiments *N*-  
33  
34 methylanilides were employed at the C-terminus. Replacing proline with the acyclic, *N*-  
35  
36 methylated amino acid, sarcosine, **21**, resulted in approximately 2-fold lower affinity than the  
37  
38 proline-containing analogue, **19c**, suggesting that relative to sarcosine, the conformational  
39  
40 constraint of proline is important. Interestingly, alanine (**22**) was equipotent to proline whereas  
41  
42 *N*-methylation of the alanine (**23**) reduced affinity 4-fold. This suggests that the Tle-Pro peptide  
43  
44 bond is likely in the *trans* conformation when bound to STAT6. Given that Xaa-Yaa peptide  
45  
46 bonds sample significant *cis* conformations when Yaa is an imino acid, such as *N*-methyl  
47  
48 alanine, the lower affinity of **23** relative to **22** may be due to the lower effective concentration of  
49  
50 the *trans* conformer in the former.<sup>34</sup>  
51  
52  
53  
54

55 Contributions of the atoms of the C-terminal amide bond were studied by replacement  
56  
57 with conformationally constrained vinyl analogs (Table 7). Substituting the CONH group of **19d**  
58  
59  
60

1  
2  
3 with a simple carbon-carbon double bond (**24**) reduced affinity over 10-fold. Extending the  
4  
5 aliphatic chain by two methylene groups (**25**) increased affinity to 0.5  $\mu\text{M}$ . Reduction of the  
6  
7 vinyl group of **25** to an alkane (**26**) resulted in a slight decrease in affinity. Reduction of the  
8  
9 carbonyl group of the methyl,phenyl amide of **19c** resulted in a four-fold loss in affinity (**27**).  
10  
11 Thus the carbonyl and nitrogen atoms of the C-terminal amide contribute to affinity for the SH2  
12  
13 domain of STAT6.  
14  
15

### 16 17 18 **Computed structure of 18a bound to the SH2 domain of STAT6.**

19  
20 To date our attempts to crystallize STAT6 either alone or in the presence of a  
21  
22 phosphopeptide have not been successful. To elucidate potential interactions between **18a** (the  
23  
24 phosphate analog of **17**) and STAT6 we employed a molecular modeling strategy that combines  
25  
26 an AutoDock-based incremental protocol of flexible protein-ligand docking (DINC) and  
27  
28 molecular dynamics simulations.<sup>35, 36</sup> A homology model of STAT6, based on the template  
29  
30 structure of STAT1 (PDB ID 1YVL, chain A), was obtained from ModBase.<sup>37</sup> Using DINC,<sup>35</sup>  
31  
32 **18a** was docked to the SH2 domain of STAT6. The complex was submitted to molecular  
33  
34 dynamics simulation in explicit water. We obtained five clusters through k-mean clustering  
35  
36 (k=5). The sizes of the clusters were 173, 115, 101, 59, and 52 frames. Throughout the  
37  
38 simulation, RMSD variations of **18a** were largely between 1 and 2.5 Å indicating that the peptide  
39  
40 mimetic in the complex was stable. In the computed models, the inhibitor interacts with the  
41  
42 surface of the protein and there do not appear to be deep pockets (Figures 3A and 3B).  
43  
44 Hydrogen bonds are illustrated in the interaction diagram of Figure 3C and the stereo rendering  
45  
46 in Figure 3D. The phosphate participates in ionic interactions with Lys544 and Arg562 and  
47  
48 hydrogen bonding interactions with the main chains of Asp565 and Ser566, which are analogous  
49  
50 to phosphate interactions with STAT1<sup>38, 39</sup> and STAT3<sup>40</sup> observed in x-ray crystallographic  
51  
52 structures and computational models of phosphopeptides bound to STAT3.<sup>28, 36</sup> These hydrogen  
53  
54  
55  
56  
57  
58  
59  
60

1  
2  
3 bonds were very stable and were present in greater than 90% of the trajectory frames throughout  
4  
5 the molecular dynamics simulation. The exception was the interaction between O2 of the  
6  
7 phosphate and one of the guanidino NH<sub>2</sub> groups of Arg562 (75% of trajectory frames). The  
8  
9 hydrogen bond between the NH of Tle and the main chain C=O of Asn588 is typical of  
10  
11 phosphopeptide interactions with SH2 domains and was present in 83% of the trajectory frames.  
12  
13 Also noted was a very stable hydrogen bond between the C=O of Tle and the main chain NH of  
14  
15 Gln590 (100% of trajectory frames). Interactions between the C=O of the pY+1 residue and the  
16  
17 NH of Glu638 (analogous to Gln590) were also seen in computed models of phosphopeptides  
18  
19 bound to STAT3.<sup>36,41</sup> The aryl group of the cinnamate and the C-terminal iodophenyl group  
20  
21 “sandwich” the side chain of Gln590, which extends away from the protein surface (Figures 3A,  
22  
23 3B, and 3D). Not surprisingly, there were several hydrophobic interactions with the SH2 domain  
24  
25 of STAT6, which are depicted as orange surfaces in Figure 3A and which are summarized in the  
26  
27 interaction diagram in Figure 3C. The *tert*-butyl group of Tle interacts with the side chain  
28  
29 methylene groups of Glu587 and the side chain of His 575. The C-terminal benzene rings  
30  
31 interact with a hydrophobic surface comprised of the side chains of Ile589, Phe592, Leu609,  
32  
33 Leu612, Ile606 and the side chain CH<sub>2</sub> groups of Arg605. This hydrophobic surface does not  
34  
35 appear to be able to accommodate the side chain benzene ring of Phe at position pY+3 in the  
36  
37 peptides, which is extended from the proline by the  $\alpha$  and  $\beta$  carbons. Thus the peptides exhibit  
38  
39 lower affinity than the mimetics.  
40  
41  
42  
43  
44  
45  
46  
47  
48  
49  
50  
51  
52  
53  
54  
55  
56  
57  
58  
59  
60

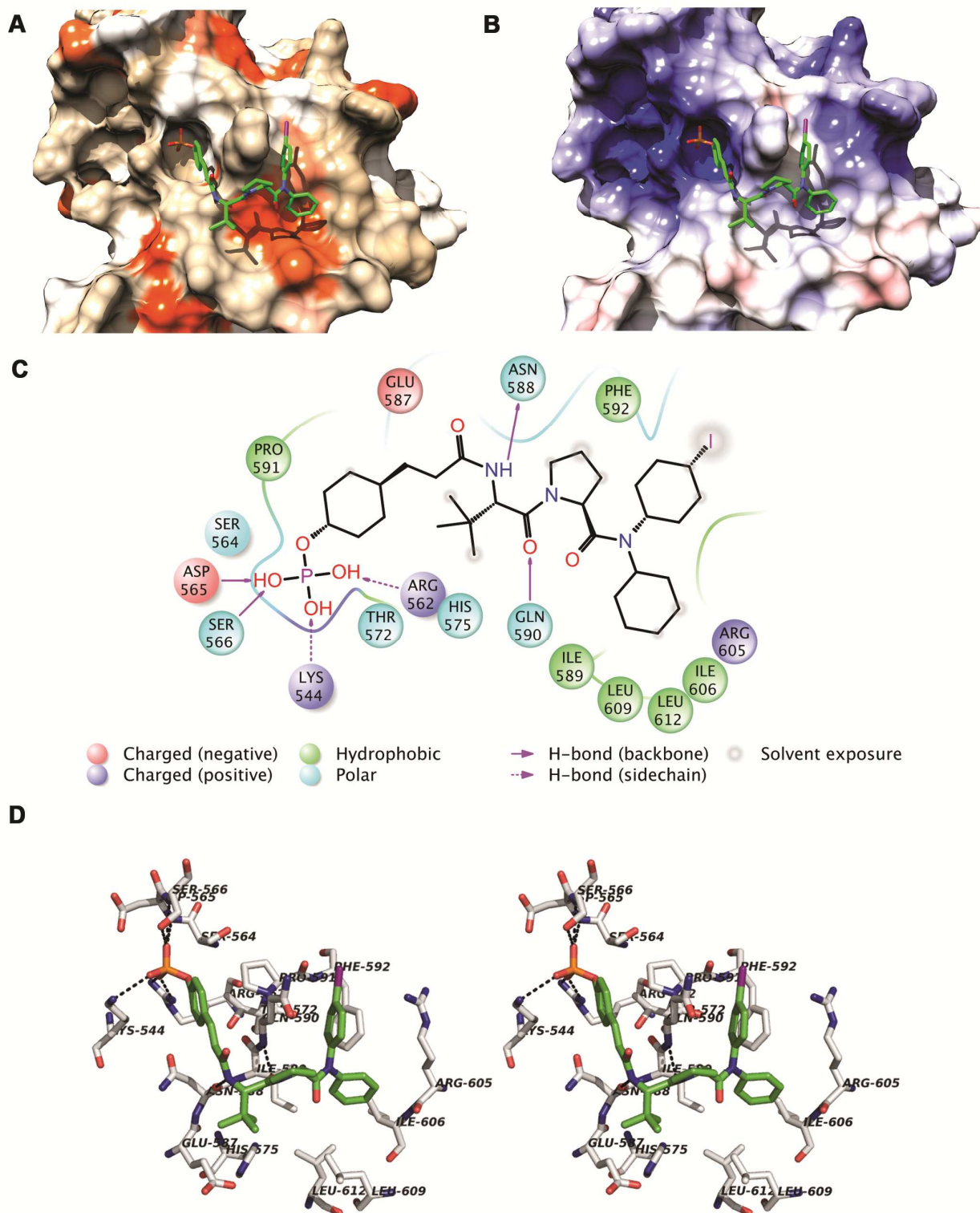


**Figure 3.** Computed structure of **18a** in complex with a homology model of STAT6. A representative complex from the largest cluster from the final 10 ns of a molecular dynamics

1  
2  
3 simulation is shown (see Methods). A. STAT6 (comprised of the linker and SH2 domains) is  
4 shown in surface representation with coloring according to amino acid hydrophobicity on Kyte-  
5 Doolittle scale B. STAT6 is shown in surface representation with coloring according to APBS-  
6 based electrostatic potentials. C. Intermolecular interaction diagram showing interactions  
7 between **18a** and amino acids from the SH2 domain of STAT6. Structures in A and B were  
8 drawn using Chimera software, C was drawn using Maestro/Schrödinger software, and D was  
9 rendered in PyMOL.  
10  
11  
12  
13  
14  
15  
16  
17  
18  
19  
20  
21

### 22 **Inhibition of Stat6 phosphorylation in intact cells with prodrugs derived from**

23 **phosphopeptide mimetics.** A set of analogs of **17** (Chart 1) was synthesized to systematically  
24 evaluate the effect of structural modifications on the ability to inhibit STAT6  
25 phosphorylation in intact cells (Figure 4). Beas-2B immortalized human airway epithelial  
26 cells were incubated with prodrugs for 2 h and stimulated with IL-4 for 1 h. Levels of pSTAT6  
27 and total STAT6 proteins were evaluated by western blotting of the cell lysates. The first series  
28 was a set of analogs of phosphates **18a-d**. Starting with **17**, possessing a phenyl, 4-iodophenyl  
29 amide, we removed the iodine (**28**), and then replaced one of the phenyl rings with a methyl  
30 group (**29**) then a hydrogen (**30**). As depicted in Figure 4A, removing the iodine from **1** resulted  
31 in a dramatic increase in potency (**28**). Significant inhibition was observed at 100 nM and  
32 complete inhibition occurred at 500 nM. Substitution of one of the phenyl groups with a methyl  
33 group (**29**) produced a further increase in potency with significant inhibition at 50 nM and nearly  
34 complete inhibition at 100 nM. Replacing the methyl group with a hydrogen (**30**), resulted in  
35 approximately 25-fold less potency. Cellular viability (MTS assay, 72 h exposure, Figure 4C)  
36 did not parallel potency for STAT6 inhibition. The trend NPh,PhI < NPh<sub>2</sub> < NMePh < NHPH  
37 indicates that smaller amides result in greater cytotoxicity. At concentrations ≤1 μM, diphenyl  
38  
39  
40  
41  
42  
43  
44  
45  
46  
47  
48  
49  
50  
51  
52  
53  
54  
55  
56  
57  
58  
59  
60

amide **28** and methylanilide **29** did not affect viability although pSTAT6 was completely inhibited. Thus for these compounds, the reason for the observed cytotoxicity is not STAT6 phosphorylation inhibition. In contrast, for **30**, the fraction of viable cells paralleled pSTAT6 inhibition. These results suggest that the C-terminal anilide is engaged in an as yet undefined off-target interaction that produces a cytotoxic effect.

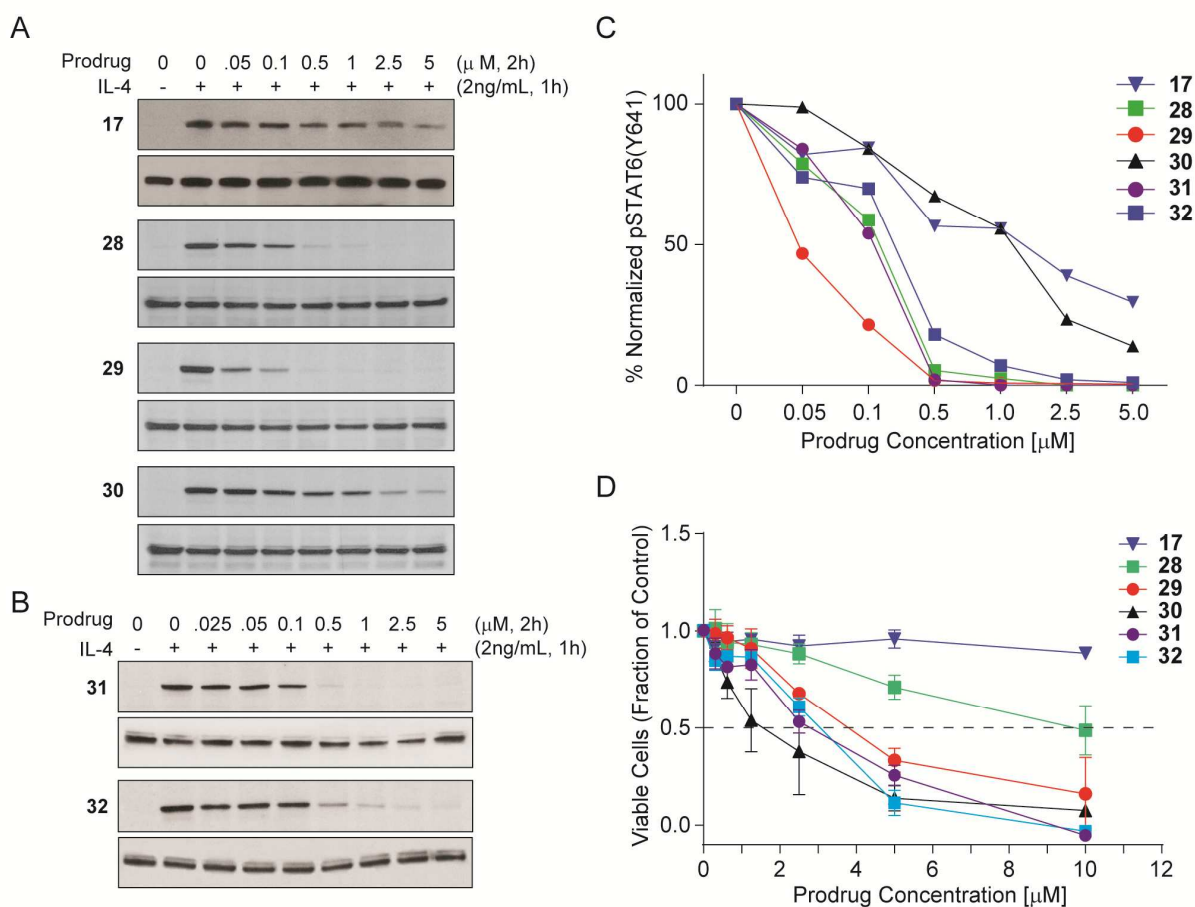


**Figure 4.** Effect of structure on inhibition of pSTAT6 and cytotoxicity. Bease-2B immortalized human epithelial airway cells were treated with the prodrugs for two h and were then stimulate with IL-4 for 1 h. Cells were lysed and total and phosphorylated STAT6 were estimated by western blots. For each pair of gels the top is pSTAT6 and the bottom is total STAT6. A. Prodrugs with cinnamoyl pTyr mimics. B. Prodrugs with  $\beta$ -methyl pTyr mimics. C. Graphic

1  
2  
3 representation the integrals of the bands in A and B. D. Effect of prodrugs on viability of Beas-  
4  
5 2B cells. Cells were treated with the prodrugs for 72 hr and viability was measured with MTT  
6  
7 assays.  
8  
9

10  
11  
12 A second set of prodrugs was prepared to test the effect of  $\beta$ -methyl substitution on the  
13  
14 cinnamate on cellular activity, as this substitution produced a small but significant increase in  
15  
16 affinity of the phosphate analogs. Figure 4B shows that **31**, the analog of **29**, retains potency and  
17  
18 the  $\beta$ -methyl group has no noticeable effect on inhibition of pSTAT6. In **32** a cyclohexyl,methyl  
19  
20 amide group replaced the phenyl,methyl amide of **31**. As can be seen this substitution also  
21  
22 resulted in high potency. Cell viabilities of **31** and **32** were nearly identical to that of **29**. Thus  
23  
24 the  $\beta$ -methyl group has no effect on cytotoxicity in this cell line.  
25  
26  
27  
28  
29

30  
31 Interestingly, cellular potency did not parallel affinity for STAT6 of the corresponding  
32  
33 phosphates, **18a-d**, and **19c**, and **19g**. Whereas affinity of the phosphate series decreased with  
34  
35 decreasing aromatic character or decreasing methyl substitution, this was not the defining feature  
36  
37 for the prodrug potency. Similar observations were made in the case of our prodrugs targeted to  
38  
39 the SH2 domain of STAT3. For example, changing the C-terminal CONHBn to a simple methyl  
40  
41 group in one series reduced affinity by a factor of two but increased cellular potency of the  
42  
43 prodrug by 50-fold.<sup>31</sup> In another series, substitution on the ring of a proline had no effect on  
44  
45 affinity but increased cellular potencies from 20-100 $\times$ .<sup>42</sup> Thus, for this class of phosphonate  
46  
47 prodrugs, biochemical affinity of the ligand for the target SH2 domain is not linearly predictive  
48  
49 of cellular activity.  
50  
51  
52  
53  
54  
55

56 **Other cell lines and other SH2 domains.**  
57  
58  
59  
60

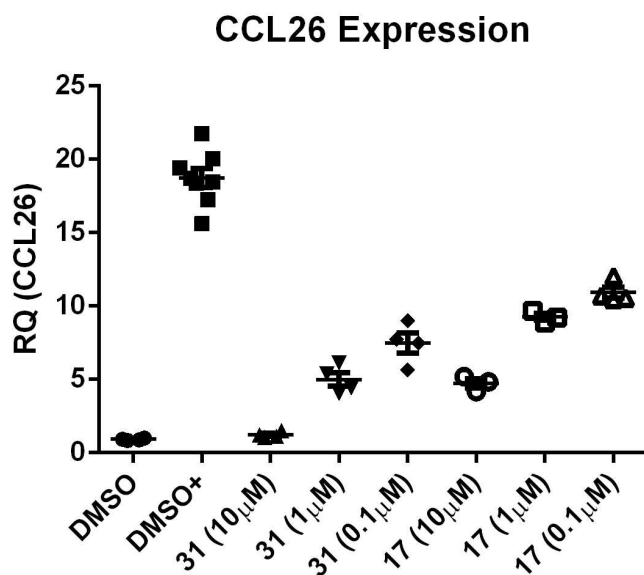
1  
2  
3 The panel of prodrugs was tested for pSTAT6 inhibition in the triple negative breast cancer cell  
4 line, MDA-MB-468. After serum starvation, cells were treated with prodrugs followed by IL-4  
5 stimulation which resulted in pSTAT6 inhibition. Overall the pattern of inhibition paralleled that  
6 of the Beas-2B epithelial airway cells (Supplemental Figure 1). Treatment of serum starved  
7 MDA-MB-468 cells with epidermal growth factor (EGF) activates the PI3K pathway leading to  
8 AKT phosphorylation,<sup>43</sup> a process that is initiated by binding of the SH2 domain of p85, the  
9 regulatory subunit of PI3K, to pTyr residues on the EGF receptor.<sup>44</sup> There was no clear trend for  
10 inhibition of pAkt as a function of structure. Whereas most compounds had no effect, **29** and **31**  
11 exhibited mild inhibition at the relatively high concentration of 5  $\mu$ M. The exception was anilide  
12 **30**, which potently inhibited pAkt at concentrations as low as 100 nM. MTS assays showed that  
13 for the panel of prodrugs, IC<sub>50</sub> values for this cell line ranged from 5 – 10  $\mu$ M. It is unclear if the  
14 decrease in pAkt is due to cross reactivity with the SH2 domains of p85 or due to other non-  
15 related off-target effects that might affect this pathway.  
16  
17  
18  
19  
20  
21  
22  
23  
24  
25  
26  
27  
28  
29  
30  
31  
32  
33

34 The panel of prodrugs was assayed for the ability to inhibit the phosphorylation of  
35 STAT1, STAT3, STAT5 and STAT6 in primary mouse CD4<sup>+</sup> T lymphocytes (Supplementary  
36 Figure 2). Similarly to Beas-2B cells, inhibition of IL-4 stimulated pSTAT6 with **17** was  
37 relatively weak and the others stronger. We further found robust inhibition of IL-2 mediated  
38 STAT5 phosphorylation after treatment with **29**, **28**, **31** and **32**. This is not surprising given the  
39 high homology in the SH2 domains of these two proteins. The hydrophobic surface mentioned  
40 above for STAT6 (Ile589, Phe592, Arg605, Ile606, Leu609, and Leu612) is highly homologous  
41 in STAT5 (L643, Phe646, Arg661, Leu662, Leu665, and Leu668). The side chain CH<sub>2</sub> groups  
42 of Lys644 in STAT5 can also contribute to the hydrophobic binding site in an analogous manner  
43 to that of Gln590 in STAT6. Interestingly, anilide **30** showed selectivity for STAT6 as it was not  
44  
45  
46  
47  
48  
49  
50  
51  
52  
53  
54  
55  
56  
57  
58  
59  
60

an inhibitor of pSTAT5. None of the prodrugs affected the phosphorylation status of STAT1 or STAT3.

### Inhibition of the expression of CCL26 (eotaxin-3)

Starting prodrug **17** and analog **31** were tested for their ability to inhibit the expression of the downstream gene, CCL26 (eotaxin-3), a chemokine involved in the recruitment of eosinophils to sites of inflammation.<sup>45, 46</sup> Beas-2B cells were treated with the inhibitors and after 24 h of exposure to IL-13, expression of CCL26 mRNA was assessed by quantitative PCR. As can be seen in Figure 5, addition of IL-13 led to robust expression of CCL26 mRNA (DMSO+). The expression of CCL26 mRNA was inhibited in a dose dependent manner by both prodrugs. In both cases, >50% inhibition was achieved at 100 nM. The greater potency of **31** reflects its greater ability to inhibit STAT6 phosphorylation than **17**. Thus steric block of the STAT6 SH2 domain with these prodrugs not only inhibits activation (phosphorylation of Tyr641), it inhibits subsequent transcriptional activity.



1  
2  
3 **Figure 5.** Prodrugs targeting the SH2 domain of STAT6 inhibit the expression of CCL26  
4 mRNA. Beas2B cells plated at  $4 \times 10^5$  cells/well and incubated overnight in complete media,  
5  
6 serum starved for 2hr, pre-treated with drug for 2hr, stimulated with IL-13 overnight in serum  
7  
8 free media, and total CCL26 mRNA was quantitated on cell lysates.  
9  
10  
11  
12  
13

## 14 15 **Chemistry**

16  
17 **Phosphopeptide Synthesis.** Phosphopeptides in Tables 1 - 3 were synthesized by manual solid  
18 phase techniques using the Fmoc protection scheme. C-termini were prepared as amides by the  
19 employment of Rink amide resin. N-termini were capped with acetyl groups unless otherwise  
20 noted. Phosphotyrosine was introduced as the phosphoro-bis-dimethylamide.<sup>47-49</sup> For the 5-  
21 phosphoryloxyindole (**15**) and 5-phosphoryloxybenzofuran-2-carboxylates (**16**), the  
22 corresponding 5-hydroxy-2-carboxylates were coupled to resin-bound peptides and were  
23 phosphorylated using global phosphorylation with *N,N*-diisopropyl-di-*tert*-butylphosphoramidite  
24 in the presence of <sup>1</sup>*H*-tetrazole. Peptides terminating in 4-phosphoryloxybenzamide and 4-  
25 phosphoryloxy- $\beta$ -methylcinnamide were capped with the corresponding phosphorylated  
26 cinnamic acid-pentachlorophenyl esters as described previously.<sup>28</sup> Peptides were cleaved from  
27 the resin using TFA:TIS:H<sub>2</sub>O.<sup>50</sup> Peptides containing phosphoro-bis-dimethylamides were left  
28 overnight to de-amidate the phosphate group.<sup>47-49</sup> All phosphopeptides were purified by reverse  
29 phase HPLC and were the correct molecular weight as measured by electrospray mass  
30 spectrometry.  
31  
32  
33  
34  
35  
36  
37  
38  
39  
40  
41  
42  
43  
44  
45  
46  
47  
48  
49

50 **Synthesis of phosphate analogs of 17.** We used convergent synthesis methodology to prepare  
51 phosphates for analysis of affinity for STAT6 protein in which modified dipeptides were  
52 synthesized and coupled to pre-formed constrained phosphotyrosine surrogates. For inhibitors  
53  
54  
55  
56  
57 **18-20** possessing constrained cinnamate and indole-based pTyr mimics (Table 4), diphenyl and  
58  
59  
60

1  
2  
3 phenyl,4-iodophenyl amines were not amenable to simple coupling to Boc-proline (**33**). In these  
4 cases the first aryl group was installed as the anilide or 4-iodophenylamide of Boc-Pro-OH using  
5 water soluble EDC as the coupling agent (**34a, b**) (Scheme 1). The second phenyl group was  
6 added by treatment with triphenylbismuth in the presence of cupric acetate and triethyl amine  
7 (**35a, b**).<sup>51, 52</sup> The Boc group was removed with TFA and the resulting amine was coupled to  
8 Boc-*tertiary*-leucine with HBTU (**36a** and **36b**). Again the Boc group was removed to give  
9 dipeptide amine salts **37a** and **37b**. Intermediate **37a** was capped with pentachlorophenyl 4-  
10 phosphoryloxycinnamate (**38a**)<sup>28</sup> and pentachlorophenyl  $\beta$ -methyl-4-phosphoryloxycinnamate  
11 (**38b**)<sup>31</sup> to give inhibitors **18a** and **19a** (Table 4), respectively. Amine **37b** was acylated with **38a**  
12 and **38b** to give **18b** and **19b**, respectively (Table 5). The alternative pTyr surrogate, 5-  
13 phosphoryloxyindole-2-carboxylate was introduced by coupling **37a** with 5-*di-tertiary*-  
14 butoxyphosphoryl-indoline-2-carboxylic acid (Scheme 2) (**39**) in presence of HBTU and DIPEA.  
15 Treatment with TFA for an hour and purification by HPLC gave **20** (Table 4).  
16  
17  
18  
19  
20  
21  
22  
23  
24  
25  
26  
27  
28  
29  
30  
31  
32  
33

34 As shown in Scheme 2, 5-*di-tertiary*-butoxyphosphoryl-indoline-2-carboxylic acid (**39**)  
35 was prepared by protection of the carboxyl group of 5-hydroxyindole-2-carboxylate (**40**) as a  
36 *tert*-butyl dimethylsilyl (TBDMS) ester (**41**) followed by phosphitylation of the hydroxyl group  
37 with *N,N*-diethyl di-*tert*-butyl phosphoramidite and subsequent oxidation to the phosphate ester  
38 with *tert*-butyl hydrogen peroxide (**42**). Aqueous hydrolysis of the TBDMS ester gave the free  
39 carboxylate, **39** ready for capping **37a** (Scheme 1).  
40  
41  
42  
43  
44  
45  
46  
47

48 Inhibitors in which the C-terminal amide was explored (**18c-d, 19c-i**, Table 5) were  
49 prepared by initial routine coupling of amines to Boc-proline using EDC (**43c-i**, Scheme 3). The  
50 Boc group was removed with TFA and Boc-*tertiary*-leucine was coupled with HBTU (**44c-i**).  
51 Again the Boc group was removed and the dipeptides were capped with **38a** or **38b** to give  
52 inhibitors **18c-d** and **19c-i**.  
53  
54  
55  
56  
57  
58  
59  
60

1  
2  
3 Inhibitors **21** – **23** (Table 6), in which proline was replaced with non-constrained  
4 sarcosine, alanine, and *N*-methylalanine, respectively, were prepared by simple coupling of *N*-  
5 methylalanine to the corresponding Boc-amino acid and elaborating as in Scheme 3.  
6  
7

8  
9  
10 Inhibitors **24-27** (Table 7) were synthesized to establish the importance of the C-terminal  
11 amide bond. As shown in Scheme 4, (*S*)-2-styryl-*N*-Boc-pyrrolidine (**46**) and (*S*)-2-(3-phenyl-  
12 propenyl)-*N*-Boc-pyrrolidine (**48**) were synthesized through a Wittig olefination of Boc-Proline  
13 (**45**) and the corresponding triphenylphosphonium bromide derivative. Fully reduced (*S*)-2-(4-  
14 phenylbutyl)-*N*-Boc-pyrrolidine (**50**) was obtained by hydrogenation of **48** in presence of  
15 10%Pd-C. An analog with a reduced amide bond was prepared by consecutive reductive-  
16 amination of Boc-proline with aniline (**52**) and then with formaldehyde (40% solution) (**53**).  
17 Intermediates **46**, **48**, **50** and **53** were elaborated to dipeptide amines **47**, **49**, **51** and **54** by TFA-  
18 mediated acidolysis of the Boc protecting group, HBTU-mediated coupling with Boc-Tle-OH,  
19 and then Boc cleavage with TFA as in Scheme 3. Treatment of the amine salts with **39b** gave  
20 inhibitors **24-27**.  
21  
22  
23  
24  
25  
26  
27  
28  
29  
30  
31  
32  
33  
34  
35

36 Cell permeable prodrugs (Chart 1) were synthesized (Scheme 5) by coupling dipeptide  
37 amines to pentachlorophenyl active esters of bis-POM protected  
38 phosphonodifluoromethylcinnamates **55a** or **b**, that were synthesized as described previously.<sup>31, 32</sup>  
39 Couplings were carried out in NMP in the presence of *N*-methylmorpholine with DMAP  
40 catalysis. Products were purified by reverse phase HPLC with gradients of MeCN in H<sub>2</sub>O with  
41 no additives in the mobile phase.  
42  
43  
44  
45  
46  
47  
48  
49

## 50 Conclusions

51 The sequence surrounding Tyr631, the docking site of IL-4R $\alpha$ , binds weakly to STAT6. This  
52 contrasts with STAT3 where a peptide derived from the docking site on gp130 (Tyr904) had low  
53 nM affinities.<sup>53, 54</sup> In the modified dipeptides reported by McKinney et al.<sup>23, 24</sup> the aryl groups at  
54  
55  
56  
57  
58  
59  
60

1  
2  
3 pY+3 were closer to the main chain than the phenyl group of phenylalanine in the  
4  
5 phosphopeptide series. Whereas C-terminal aryl amides produced the highest affinity, low nM  
6  
7 binding constants could also be obtained with *N*-methyl anilides and di-alkyl amides. The  
8  
9 smaller hydrophobic groups of the latter likely do not penetrate as deeply into the proposed  
10  
11 hydrophobic pocket as do benzene rings. Cellular potency of the bis-POM prodrugs was  
12  
13 dependent on the substituents of the C-terminal amide but did not parallel affinity for STAT6 by  
14  
15 the corresponding phosphates. Cellular activity of a peptidomimetic or any other drug is a  
16  
17 function of many factors that may include 1, the intrinsic affinity of the drug for its target (e.g.  
18  
19 enzyme, transcription factor, miRNA); 2, effectiveness of cell penetration; 3, efflux from the  
20  
21 cell; 4, metabolic stability; 5, partitioning into membranes versus the cytosol, and other possible  
22  
23 interactions. It is not clear which of these factors contributes to the deviation in cellular potency  
24  
25 of the prodrugs from affinity for STAT6 of the corresponding phosphates. Inhibition of cell  
26  
27 viability was inversely proportional to the size of the C-terminal amide with the smaller  
28  
29 methylanilide and anilide analogs being most inhibitory. These apparent off-target effects can  
30  
31 potentially induce more than one type of biological response in vivo and it will be necessary to  
32  
33 carefully monitor toxicity in animal studies. The prodrugs were quite potent in inhibiting  
34  
35 expression of CCL26, suggesting that this class of compounds will have utility in modulating  
36  
37 immune responses. In the case of asthma, cytotoxicity is detrimental so care will have to be  
38  
39 exercised to achieve the therapeutic window. The inhibitors were selective for STAT6 over  
40  
41 STAT1 and STAT3. The basis of the selectivity can be explained as follows. At the base of the  
42  
43 hydrophobic pocket that accommodates the C-terminal aromatic groups in STAT6 is Phe592. In  
44  
45 the sequences of STAT1, STAT2, STAT3, and STAT4, the corresponding residue is a tyrosine.  
46  
47 In the crystal structure of a phosphopeptide bound to STAT1,<sup>39</sup> and in models calculated for  
48  
49 phosphopeptide-STAT3 complexes,<sup>28, 36, 41</sup> the side chain hydroxide of this tyrosine contacts a  
50  
51  
52  
53  
54  
55  
56  
57  
58  
59  
60

1  
2  
3 main chain peptide bond in a hydrogen bond which appears to be part of the recognition  
4  
5 determinant for these SH2 domains. Based on these models, this hydroxyl group, and associated  
6  
7 waters of hydration, in STAT1 and STAT3 would repel the C-terminal amide aromatic groups of  
8  
9 the inhibitors, thus leading to selectivity for STAT6 (and STAT5). The observed cross reactivity  
10  
11 to STAT5 in asthma is not likely to be a problem in clinical settings. As STAT5 was reported to  
12  
13 be required for the asthma phenotype in a STAT6-independent manner,<sup>55</sup> cross reactivity to  
14  
15 STAT5 may actually contribute to in vivo efficacy. Evaluation of prodrugs in a fungal-induced  
16  
17 murine model of asthma is in progress and will be reported under separate cover.  
18  
19  
20  
21  
22  
23

## 24 **Methods**

25  
26 N<sup>a</sup>-protected amino acids were purchased from, ChemImpex, or NovaBiochem. HOBt was  
27  
28 from ChemImpex. For the synthesis of phosphopeptides, Rink resin (Advanced Chemtech, Inc.)  
29  
30 with a loading of 0.6 mmol/gm was employed. Anhydrous DMF for amino acid solutions, and  
31  
32 aniline derivatives were from Aldrich. Other solvents were reagent grade and were used without  
33  
34 further purification. NMR spectra were obtained on either a Bruker DPX 300 MHz spectrometer  
35  
36 or a Bruker DRX 500 MHz spectrometer.  
37  
38  
39

40  
41 **General Procedure for the synthesis of phosphopeptides.** Solid phase syntheses were carried  
42  
43 out manually using commercially available Rink resin. Resin, 0.2 gm, was placed in a manual  
44  
45 reactor and swollen and washed with 5 × 10 mL of DMF/CH<sub>2</sub>Cl<sub>2</sub>. Fmoc groups were removed  
46  
47 with 3 × 6 mL of 20% piperidine/DMF for 5 min each. For coupling, three-fold excesses of  
48  
49 Fmoc-amino acids, DIC, and HOBt were used in 8-10 mL of DMF/CH<sub>2</sub>Cl<sub>2</sub> and were allowed to  
50  
51 proceed until resin samples tested negative with ninhydrin tests. After coupling and deprotection  
52  
53 steps, resins were washed with 5 × 10 mL of DMF/CH<sub>2</sub>Cl<sub>2</sub>. On completion of the peptide chain,  
54  
55 resins were washed with CH<sub>2</sub>Cl<sub>2</sub> (3 × 10 mL) and were treated with TFA: TIS: H<sub>2</sub>O (95:2.5:2.5)  
56  
57  
58  
59  
60

1  
2  
3 (3 × 5 mL) for 15 min each. The combined filtrates volumes were reduced in vacuo. Peptides  
4  
5 were precipitated in Et<sub>2</sub>O and collected by centrifugation. After drying, peptides were purified by  
6  
7 reverse phase HPLC on a Varian Dynamax HPLC using a Phenomenex Luna C18 (2) 10 μM, 2.1  
8  
9 x 25 cm column. Gradients of 0.1% TFA-MeCN in 0.1% TFA-H<sub>2</sub>O with a flow rate of 20  
10  
11 mL/min were employed. For prodrugs, no TFA was used in the mobile phase. Peptides were  
12  
13 tested for purity by reverse phase HPLC on a Waters Alliance HPLC using a Phenomenex Luna  
14  
15 C18 (2) 5μM 2.1 x 250 mm column at a flow rate of 0.4 mL/min. A gradient of 0-40%  
16  
17 MeCN/30 min was used for phosphopeptides and peptide intermediates. For prodrugs the  
18  
19 gradient was 10-80% MeCN/30 min. Phosphopeptides and prodrug intermediates were dried in  
20  
21 vacuo over P<sub>2</sub>O<sub>5</sub> at 37° for 24 h prior to use.<sup>53</sup> All compounds were >95% pure (HPLC) before  
22  
23 evaluation. Purities, yields, and mass spectral characteristics of phosphopeptides and prodrugs  
24  
25 are provided in the supporting information.  
26  
27  
28  
29  
30  
31

32 **Synthesis of 4-(di-*tert*-butoxyphosphoryloxy)-Indole-2-carboxylic acid, 40:** To a  
33  
34 suspension of 5-hydroxyindole-2-carboxylic acid (1.0 g, 5.64 mmol) and *tert*-butyldimethylsilyl  
35  
36 chloride (0.85g, 5.64 mmol) in 10 mL of dry THF, *N*-methyldimorpholine (0.62 mL, 5.64 mmol)  
37  
38 was added at room temperature. After 15 min, 1*H*-tetrazole (1.6 g, 22.56 mmol) was added in  
39  
40 one portion followed by the addition of di-*tert*-butyl *N,N*-diethylphosphoramidite (3.9 g, 11.3  
41  
42 mmol) in 15 mL of dry THF. After stirring for 2 h, 70% aq. *tert*-butylhydroperoxide (3.0 mL,  
43  
44 16.9 mmol) was added at 0°C and the mixture was stirred for 2 h more. The reaction was  
45  
46 quenched with slow addition of an aqueous solution of 10% Na<sub>2</sub>S<sub>2</sub>O<sub>5</sub> and stirred for 1.0 h. It was  
47  
48 then diluted with ethyl acetate (30 mL) and extracted with an additional amount of ethyl acetate  
49  
50 (2 × 20 mL). The combined organic parts were washed with water followed by brine and dried  
51  
52 (MgSO<sub>4</sub>). Solvent was removed and the crude product was triturated with hexane-ether. The  
53  
54 product was collected by filtration and dried to give 1.5 g (71%) of a white solid, which was used  
55  
56  
57  
58  
59  
60

1  
2  
3 without further purification.  $^1\text{H}$  NMR (DMSO- $d_6$ , 300 MHz)  $\delta$  1.26 (s, 18H), 6.88-6.94 (m, 2H),  
4  
5  
6 7.21-7.26 (m, 2H), 11.62 (s, 1H).  $^{13}\text{C}$  NMR (DMSO- $d_6$ , 75 MHz)  $\delta$  29.9, 83.1, 83.2, 107.8,  
7  
8 112.0, 113.6, 118.5, 127.3, 130.1, 134.8, 145.2, 145.3, 163.1. MS (ESI)  $m/z$  : (M+1) $^+$  calcd:  
9  
10 370.3; found 370.4.

### 11 12 13 **General procedure for Boc-prolinamide formation:**

14  
15 A solution of Boc-proline (1.0 g, 4.64 mmol), the appropriate amine (1.0 equiv) and EDC (1.2  
16  
17 equiv) in 60 mL of dry dichloromethane was stirred for overnight. It was then transferred to a  
18  
19 separatory funnel with an additional 20 mL of  $\text{CH}_2\text{Cl}_2$  and washed with 5% HCl (2  $\times$  30 mL)  
20  
21 followed by 10%  $\text{NaHCO}_3$  (2  $\times$  30 mL) and brine (1  $\times$  20 mL). The organic layer was dried  
22  
23 (MgSO $_4$ ) and concentrated under reduced pressure. The residue was used as such for the next  
24  
25 step or purified by flash chromatography with gradients of EtOAc in hexanes.  
26  
27

28  
29  
30 Boc-Pro-NHPhI, **34a**<sup>33</sup>

31  
32 **Boc-Pro-NHPh, 34b:** Yield 1.2 gm, 90%, starting from 4.64 mmol of Boc-Proline.  $^1\text{H}$ -NMR  
33  
34 (300 MHz,  $\text{CDCl}_3$ )  $\delta$  1.5 (s, 9H), 1.91-1.95 (m, 3H), 2.52 (m, 1H) 3.44 (m, 2H), 4.44(m, 1H), 7.1  
35  
36 (m, 1H), 7.3 (t, J = 7.6 Hz, 2H), 7.5 (d, J = 8.0 Hz, 2H), 9.5 (brs, 1H). MS (ESI)  $m/z$  : (M+23) $^+$   
37  
38 calcd: 313.2; found 313.3

39  
40  
41 **Boc-Pro-N(Me)Ph, 43c:** Yield 1.1 gm, 78%, starting from 4.64 mmol of Boc-Proline.  $^1\text{H}$ -NMR  
42  
43 (300 MHz,  $\text{CDCl}_3$ )  $\delta$  1.45 (s, 9H), 1.48(isomer, s, 9H), 1.65-2.0 (m, 4H), 3.28 (s, 3H), 3.3-3.47  
44  
45 (m, 1H), 3.5-3.6 (m, 1H), 4.14 (m, 1H), 4.3 (isomer, m, 1H), 7.2-7.47 (m, 5H). MS (ESI)  $m/z$  :  
46  
47 (M+23) $^+$  calcd: 327.2; found 327.3.

48  
49  
50 **Boc-Pro-NHCH $_2$ Ph, 43e:** Yield 1.3 gm, 92%, starting from 4.64 mmol of Boc-Proline.  $^1\text{H}$ -  
51  
52 NMR (300 MHz,  $\text{CDCl}_3$ )  $\delta$  1.4 (s, 9H), 1.82-1.98 (m, 2H), 2.1-2.43 (m, 2H), 3.4 (m, 2H), 4.2-  
53  
54 4.65 (m, 3H), 6.4 (brs, 1H), 7.24-7.34 (m, 5H). MS (ESI)  $m/z$  : (M+23) $^+$  calcd: 327.2; found  
55  
56 327.3.  
57  
58  
59  
60

**Boc-Pro-NHCH<sub>2</sub>CH<sub>2</sub>Ph, 43f:** Yield 1.2 gm, 85%, starting from 4.64 mmol of Boc-Proline. <sup>1</sup>H-NMR (300 MHz, CDCl<sub>3</sub>) δ 1.42 (s, 9H), 1.74-1.9 (m, 2H), 1.95-2.4 (m, 2H), 2.7-2.9 (m, 2H), 3.27-3.4 (m, 2H), 3.4-3.6 (m, 2H), 4.22 (m, 1H), 7.2-7.33 (m, 6H). MS (ESI) m/z : (M+23)<sup>+</sup> calcd: 341.2; found 341.3.

**Boc-Pro-N(Me)C<sub>6</sub>H<sub>11</sub>, 43g:** Yield 1.1 gm, 76%, starting from 4.64 mmol of Boc-Proline. <sup>1</sup>H-NMR (300 MHz, CDCl<sub>3</sub>) δ 1.05-1.2 (m, 1H), 1.25-1.48 (m, 14H), 1.5-1.73 (m, 4H), 1.74-2.25 (m, 6H), 2.8 (s, 1.5H), 2.9 (s, 1H), 2.92 (s, 1H), 3.4-3.7 (m, 2H), 4.4 (m, 0.5H), 4.5 (m, 0.5H), 4.65 (m, 0.5H). MS (ESI) m/z : (M+23)<sup>+</sup> calcd: 333.2; found 333.3

**Boc-Pro-NMe<sub>2</sub>, 43h:** Yield 1.0 gm, 79%, starting from 4.64 mmol of Boc-Proline. <sup>1</sup>H-NMR (300 MHz, CDCl<sub>3</sub>) δ 1.4 (s, 9H), 1.46 (*isomer*, s, 9H), 1.78-1.92 (m, 4H), 1.96-2.23 (*isomer*, m, 4H), 2.96 (s, 3H), 2.97 (*isomer*, s, 3H), 3.06 (s, 3H), 3.1 (*isomer*, s, 3H), 3.4-3.5 (m, 2H), 3.53-3.66 (*isomer*, m, 2H), 4.55 (m, 1H), 4.67 (m, 1H). MS (ESI) m/z : (M+23)<sup>+</sup> calcd: 265.2; found 265.3

**Boc-Pro-NEt<sub>2</sub>, 43i:** Yield 1.1 gm, 87%, starting from 4.64 mmol of Boc-Proline. <sup>1</sup>H-NMR (300 MHz, CDCl<sub>3</sub>) δ 1.08-1.18 (m, 6H), 1.2-1.28 (*isomer*, m, 6H), 1.4 (s, 9H), 1.45 (s, 9H), 1.76-1.92 (m, 4H), 1.97-2.23 (*isomer*, m, 4H), 3.2-3.7 (m, 12H, including *isomer*), 4.45 (m, 1H), 4.6 (m, 1H). MS (ESI) m/z : (M+23)<sup>+</sup> calcd: 293.2; found 293.3

#### **General procedure for arylation of amides:** <sup>51, 52</sup>

To a stirred solution of amide **34a or b** (5.0 mmol) in dry CH<sub>2</sub>Cl<sub>2</sub> (50 mL), was added triphenylbismuth (2.0 equiv), Cu(OAc)<sub>2</sub> (2.0 equiv) and dry triethylamine (3.0 equiv). After completion of the reaction (as monitored by HPLC), the solvent was evaporated and the residue was diluted with ether (150 mL) and filtered through celite. The filtrate was then washed with 5% HCl (2 × 30 mL) followed by brine and was dried over MgSO<sub>4</sub>. Concentration under reduced

1  
2  
3 pressure followed by purification by silica gel chromatography using 10% ethylacetate-hexane  
4  
5  
6 mixture afforded the title compounds.

7  
8 **Boc-Pro-N(Ph)PhI, 35a**<sup>33</sup>

9  
10 **Boc-Pro-NPh<sub>2</sub>, 35b** Yield 0.9 gm, 71%, starting from 3.44 mmol of **35b**. <sup>1</sup>H-NMR (600 MHz,  
11  
12 CDCl<sub>3</sub>) δ 1.46 (s, 9H), 1.52 (s, 9H, *isomer*), 1.72-1.8 (m, 2H), 1.87-1.94 (m, 1H), 1.96-2.1(m,  
13  
14 5H), 3.36-3.4 (m, 1H), 3.46-3.5 (m, 1H), 3.55-3.64 (m, 2H), 4.3 (m, 1H), 4.44 (m, 1H), 7.1-7.5  
15  
16 (m, 20H, including isomer). MS (ESI) m/z : (M+23)<sup>+</sup> calcd: 389.2; found 389.3

17  
18  
19 **General procedure for dipeptide formation:**

20  
21 A solution of the appropriate Boc-prolinamide (2.0 g) in 10 mL of 95%TFA/CH<sub>2</sub>Cl<sub>2</sub> was stirred  
22  
23 for 1 h. The solution was concentrated under vacuum. Residual TFA was stripped off with by the  
24  
25 addition and evaporation of CCl<sub>4</sub> (2 × 10 mL). The residue was treated with Boc-Tle-OH (1.2  
26  
27 equiv), HBTU (1.2 equiv), and DIEA (2.5 equiv) in 50 mL of dry CH<sub>2</sub>Cl<sub>2</sub> for overnight. The  
28  
29 organic layer then diluted with an additional 50 mL of CH<sub>2</sub>Cl<sub>2</sub> and washed with 5% HCl (3 × 30  
30  
31 mL) followed by 10% NaHCO<sub>3</sub> (2 × 30 mL) and brine. After drying (MgSO<sub>4</sub>) and concentration  
32  
33 under vacuum, crude products were sufficiently pure and were used as such for the next step.

34  
35  
36  
37  
38 **Boc-Tle-Pro-N(Ph)PhI, 36a**<sup>33</sup>

39  
40 **Boc-Tle-Pro-NPh<sub>2</sub>, 36b:** Yield 0.7 gm, 77%, starting from 1.9 mmol of H-Pro-NPh<sub>2</sub>. <sup>1</sup>H-NMR  
41  
42 (600 MHz, CDCl<sub>3</sub>) δ 1.06 (s, 9H), 1.40 (s, 9H), 1.83 (m, 1H), 1.97-2.06 (m, 3H), 3.73 (m, 1H),  
43  
44 3.83 (m, 1H), 4.30 (d, J = 9.6 Hz, 1H), 4.55 (m, 1H), 5.38 (d, J = 9.6 Hz, 1H), 7.15-7.52 (m,  
45  
46 10H). MS (ESI) m/z : (M+23)<sup>+</sup> calcd: 502.3; found 502.5

47  
48  
49 **Boc-Tle-Pro-N(Me)Ph, 44c** Yield 0.69 gm, 68%, starting from 2.44 mmol of H-Pro-N(Me)Ph.

50  
51  
52 <sup>1</sup>H-NMR (600 MHz, CDCl<sub>3</sub>) δ 1.00 (s, 9H), 1.32 (s, 9H), 1.64-1.72 (m, 1H), 1.78 (m, 2H), 1.96  
53  
54 (m, 1H), 3.2 (s, 3H), 3.62 (m, 1H), 3.72 (m, 1H), 4.22 (d, J = 9.6 Hz, 1H), 4.34 (t, J = 7.4 Hz,  
55  
56  
57  
58  
59  
60

1  
2  
3 1H), 5.28 (d, J = 9.6 Hz, 1H), 7.26-7.38 (m, 5H). MS (ESI) m/z : (M+23)<sup>+</sup> calcd: 440.3; found  
4  
5 440.5  
6

7  
8 **Boc-Tle-Pro-NHPh, 44d:** Yield 0.83 gm, 79%, starting from 2.63 mmol of H-Pro-NHPh. <sup>1</sup>H-  
9  
10 NMR (600 MHz, CDCl<sub>3</sub>) δ 1.00 (s, 9H), 1.44 (s, 9H), 1.9 (m, 1H), 2.03 (m, 1H), 2.16 (m, 1H),  
11  
12 2.55 (m, 1H), 3.66 (m, 1H), 3.82 (m, 1H), 4.35 (d, J = 9.7 Hz, 1H), 4.83 (m, 1H), 5.26 (d, J = 9.6  
13  
14 Hz, 1H), 7.05 (m, 1H), 7.27 (m, 2H), 7.47 (m, 2H), 9.37 (brs, 1H). MS (ESI) m/z : (M+23)<sup>+</sup>  
15  
16 calcd: 426.3; found 426.4  
17  
18

19  
20 **Boc-Tle-Pro-NHCH<sub>2</sub>Ph, 44e:** Yield 0.72 gm, 71%, starting from 2.45 mmol of H-Pro-  
21  
22 NHCH<sub>2</sub>Ph. <sup>1</sup>H-NMR (600 MHz, CDCl<sub>3</sub>) δ 0.88 (s, 9H), 1.42 (s, 9H), 1.85-1.9 (m, 1H), 1.92-2.0  
23  
24 (m, 1H), 2.14 (m, 1H), 2.41-2.45 (m, 1H), 3.61 (m, 1H), 3.75 (m, 1H), 4.26 (d, J = 9.6 Hz, 1H),  
25  
26 4.32 (dd, J = 5.4 and 15.0 Hz, 1H), 4.46 (dd, J = 6.6 and 15.0 Hz, 1H), 4.63 (dd, J = 2.4 and 7.8  
27  
28 Hz, 1H), 5.2 (d, J = 9.6 Hz, 1H), 7.23-7.30 (m, 5H). MS (ESI) m/z : (M+23)<sup>+</sup> calcd: 440.3;  
29  
30 found 440.4  
31  
32

33  
34 **Boc-Tle-Pro-NHCH<sub>2</sub>CH<sub>2</sub>Ph, 44f:** Yield 0.53 gm, 66%, starting from 1.83 mmol of H-Pro-  
35  
36 NHCH<sub>2</sub>CH<sub>2</sub>Ph. <sup>1</sup>H-NMR (600 MHz, CDCl<sub>3</sub>) δ 0.96 (s, 9H), 1.42 (s, 9H), 1.88-1.96 (m, 2H),  
37  
38 2.06-2.09 (m, 1H), 2.28 (m, 1H), 2.74-2.81 (m, 2H), 3.47 (m, 2H), 3.61 (m, 1H), 3.77(m, 1H),  
39  
40 4.3(d, J = 9.6 Hz, 1H), 4.53 (m, 1H), 5.28 (d, J = 9.6 Hz, 1H), 6.9 (m, 1H), 7.16-7.21 (m, 3H),  
41  
42 7.27-7.3 (m, 2H). MS (ESI) m/z : (M+23)<sup>+</sup> calcd: 454.3; found 454.5  
43  
44

45  
46 **Boc-Tle-Pro-N(Me)C<sub>6</sub>H<sub>11</sub>, 44g** Yield 0.62 gm, 61%, starting from 2.38 mmol of H-Pro-  
47  
48 N(Me)C<sub>6</sub>H<sub>11</sub>. <sup>1</sup>H-NMR (600 MHz, CDCl<sub>3</sub>) δ 1.04 (s, 6H), 1.05 (s, 3H), 1.3-1.4 (m, 4H), 1.4-1.44  
49  
50 (m, 11H), 1.53-1.61 (m, 1H), 1.62-1.7 (m, 2H), 1.74-1.8 (m, 1H), 1.81-1.9 (m, 2H), 1.9-2.00 (m,  
51  
52 1H), 2.06-2.24 (m, 2H), 2.8 (s, 1H), 2.95 (s, 2H), 3.6 (m, 0.5H), 3.73 (m, 1H), 3.86 (m, 1H), 4.3-  
53  
54 4.4 (m, 1.5H), 4.83 (m, 0.5H), 4.9 (m, 0.5H), 5.35 (m, 1H). MS (ESI) m/z : (M+23)<sup>+</sup> calcd:  
55  
56 389.2; found 389.3  
57  
58  
59  
60

1  
2  
3 **Boc-Tle-Pro-NMe<sub>2</sub>, 44h** Yield 1.1 gm, 60%, starting from 4.92 mmol of H-Pro-NMe<sub>2</sub>. <sup>1</sup>H-NMR  
4  
5 (600 MHz, CDCl<sub>3</sub>) δ 1.04 (s, 9H), 1.42 (s, 9H), 1.86 (m, 1H), 1.95 (m, 1H), 2.1 (m, 1H), 2.18  
6  
7 (m, 1H), 2.94 (s, 3H), 3.11 (s, 3H), 3.74 (m, 1H), 3.86 (m, 1H), 4.33 (d, J = 9.6 Hz, 1H), 4.87 (m,  
8  
9 1H), 5.29 (d, J = 9.6 Hz, 1H). MS (ESI) m/z : (M+23)<sup>+</sup> calcd: 378.3; found 378.4

10  
11 **Boc-Tle-Pro-NEt<sub>2</sub>, 44i** Yield 1.4 gm, 64%, starting from 5.9 mmol of H-Pro-NEt<sub>2</sub>. <sup>1</sup>H-NMR  
12  
13 (600 MHz, CDCl<sub>3</sub>) δ 1.03 (s, 9H), 1.1 (t, J = 7.2 Hz, 3H), 1.27 (t, J = 7.2 Hz, 3H), 1.42 (s, 9H),  
14  
15 1.86-1.96 (m, 2H), 2.12-2.18 (m, 2H), 3.28-3.42 (m, 3H), 3.53 (m, 1H), 3.73 (m, 1H), 3.87 (m,  
16  
17 1H), 4.32 (d, J = 10.2 Hz, 1H), 4.76 (m, 1H), 5.34 (d, J = 9.6 Hz, 1H). MS (ESI) m/z : (M+23)<sup>+</sup>  
18  
19 calcd: 406.3; found 406.5

20  
21 **Synthesis of (S)-2-styryl-N-Boc-pyrrolidine, 46:**<sup>56</sup> n-BuLi (1.0 mL, 2.5 mmol) was added  
22  
23 dropwise via syringe over 10 minutes to a solution of benzyl-triphenylphosphonium bromide  
24  
25 (1.0 g, 2.3 mmol) in 20 mL of dry THF under argon at -78°C. The mixture was stirred for 1 h,  
26  
27 then Boc-L-prolinal (0.46g, 2.3 mmol) in 20 mL THF was added dropwise. The reaction was  
28  
29 allowed to stir for 24h at room temperature. The reaction mixture then quenched with 30 mL of  
30  
31 saturated NH<sub>4</sub>Cl, diluted with ethyl acetate, washed with brine (2 × 25 mL), dried over sodium  
32  
33 sulfate, and concentrated in vacuo. Silica gel chromatography (5:1 hexanes/EtOAc) yielded  
34  
35 0.480 g (76%). <sup>1</sup>H NMR (CDCl<sub>3</sub>, 300 MHz) δ 1.42 (s, 9H), 1.8-2.2 (m, 4H), 3.45 (brs, 1H), 4.3-  
36  
37 4.8 (m, 1H), 5.58-6.15 (m, 1H), 6.35-6.45 (m, 1H), 7.2-7.4 (m, 5H).

38  
39 **Synthesis of (S)-2-(4-phenyl-but-1-enyl)-N-Boc-pyrrolidine, 48:** The same procedure as  
40  
41 described for the synthesis of **46** was followed starting with 1.0 g of (3-phenylpropyl)-  
42  
43 triphenylphosphonium bromide (2.2 mmol) and 0.483 g of Boc-prolinal (2.2 mol). Yield: 0.452 g  
44  
45 (1.5 mmol, 68%). <sup>1</sup>H NMR (CDCl<sub>3</sub>, 300 MHz) δ 1.43 (s, 9H), 1.68-1.92 (m, 4H), 2.37-2.52 (m,  
46  
47 2H), 2.56-2.81 (m, 2H), 3.3-3.42 (m, 2H), 4.45 (brs, 1H), 5.27-5.45 (m, 2H), 7.14-7.31 (m, 5H).  
48  
49  
50  
51  
52  
53  
54  
55  
56  
57  
58  
59  
60

1  
2  
3 **(S)-4-phenbutyl-N-Boc-pyrrolidine, 50:** A 50-mL round-bottom flask fitted with a 3-way tap  
4 and balloon was charged with 400 mg of 10% Pd-C. The syringe and stirred for several minutes.  
5  
6 Alkene **49** (405 mg) in 5 mL EtOH was added via syringe and stirred for 2 h. Hydrogen gas was  
7  
8 added as the balloon deflated. Upon complete reaction (TLC) the catalyst was removed by  
9  
10 filtration. The product was concentrated in vacuo to yield. Colorless oil, yield 376 mg (93%). <sup>1</sup>H  
11  
12 NMR (CDCl<sub>3</sub>, 300 MHz) δ 7.15-7.31 (m, 5H), 3.70-3.76 (br m, 1H), 3.26-3.41 (m, 2H), 2.58-  
13  
14 2.64 (m, 2H), 1.59-1.93 (m, 7H), 1.49 (s, 9H), 1.30-1.35 (m, 3H).  
15  
16  
17  
18  
19

20 **Synthesis of N-Boc (S)-2-((methyl(phenyl)amino)methyl)pyrrolidine, 53.** To a stirred  
21  
22 solution of **45** (1.00 g, 5.02 mmol) and aniline (0.78 g, 6.02mmol) in MeOH:acetic acid (9:1) (10  
23  
24 mL) was added NaCNBH<sub>3</sub> (0.63 g, 10.04mmol) at room temperature. The mixture was stirred for  
25  
26 1h, evaporated to dryness and the residue extracted with AcOEt (2 x 30 mL). The organic phase  
27  
28 was washed with 5% NaHCO<sub>3</sub>, brine, dried (MgSO<sub>4</sub>) and evaporated. The product **52** (1.0 g, 3.2  
29  
30 mmol) was then dissolved in 10 mL of MeCN: acetic acid (9:1), and 37% formalin (10 mL) and  
31  
32 sodium cyanoborohydride (0.6g, 9.6 mmol) were added. The mixture was stirred for 4 h at room  
33  
34 temperature. The solution was evaporated in vacuo, the residue was dissolved in AcOEt (50 mL)  
35  
36 and was washed with 1N KOH followed by brine. The organic phase was dried (MgSO<sub>4</sub>),  
37  
38 evaporated, and the crude product was purified by silica gel chromatography using 30% EtOAc-  
39  
40 hexane mixture yielding 0.640 gm (2.2 mmol) of **53** (61%). <sup>1</sup>H NMR (CDCl<sub>3</sub>, 300 MHz) δ 1.52  
41  
42 (s, 9H), 1.8-1.95 (m, 4H), 2.98 (s, 3H), 3.0-3.21 (m, 1H), 3.28-3.48 (m, 2H), 3.56-3.72 (m,  
43  
44 1H), 4.15 (m, 1H), 6.68 (m, 1H), 6.74 -6.84 (m, 2H), 7.18-7.26 (m, 2H). MS (ESI) m/z : (M+H)<sup>+</sup>  
45  
46 calcd: 291.2; found 291.3.  
47  
48  
49  
50  
51  
52

53 **General procedure for phosphopeptide/phosphopeptidomimetic formation:** Boc-protected  
54  
55 dipeptide (0.5 g) was treated with 5.0 mL of 95% TFA-CH<sub>2</sub>Cl<sub>2</sub> for 1h. After concentration under  
56  
57 vacuum the residue was diluted with 10 mL of water, neutralized with conc. NH<sub>4</sub>OH and  
58  
59  
60

1  
2  
3 lyophilized to obtain an off-white foam. The amine was then treated with the active ester (23)  
4 (1.0 equiv) in 5 mL of dry NMP, N-methylmorpholine (NMM, 3.0 equiv) and catalytic amount  
5 of DMAP (0.05 equiv). After completion of the coupling, as monitored by HPLC, 25 mL of ether  
6 was added to the reaction mixture and the resulting emulsion centrifuged. The clear supernatant  
7 was decanted off and the crude precipitate was purified by HPLC using 0.1% TFA-MeCN-  
8 Water. Fractions containing pure phosphopeptide were combined and lyophilized to obtain pure  
9 products as white powders. Each was further dried over P<sub>2</sub>O<sub>5</sub> chamber under vacuum at 37°C  
10 before affinity measurements.<sup>53</sup> Yields, HRMS, and HPLC retention times are reported in the  
11 supporting information.  
12  
13  
14  
15  
16  
17  
18  
19  
20  
21  
22  
23

#### 24 **General procedure for prodrug formation.**<sup>31, 32</sup>

25  
26  
27 The appropriate amine, derived from a Boc-protected dipeptide as described above, was coupled  
28 with the building block **55a** or **b** (1.0 equiv) in presence of 3 mL of dry NMP, dry NMM (3.0  
29 equiv) and catalytic amount of DMAP (0.05 equiv). After completion, checked by HPLC, the  
30 product was purified by RP-HPLC using acetonitrile-water (no TFA). The pure fractions were  
31 combined and lyophilized to obtain a white powder. Yields, HRMS, and HPLC retention times  
32 are reported in the supporting information.  
33  
34  
35  
36  
37  
38  
39  
40

41 **Synthesis of  $\beta$ MpCinn-Tle-Sar-NMe(Ph), 21:** To a stirred solution of Boc-Sar-OH (2.0 g,  
42 10.6 mmol), N-methylaniline (1.2 g, 10.6 mmol), HBTU (4.8 g, 12.7 mmol) in 50 mL of dry  
43 CH<sub>2</sub>Cl<sub>2</sub>, DIEA (3.7 mL, 21.2 mmol) was added and the reaction stirred overnight. The mixture  
44 was diluted with an additional 50 mL of CH<sub>2</sub>Cl<sub>2</sub> and the solution then washed with 5% HCl (2 ×  
45 30mL) followed by 10% NaHCO<sub>3</sub> (2 × 30 mL) and brine (1 × 20 mL). The organic layer was  
46 dried (MgSO<sub>4</sub>) and evaporated to dryness under reduced pressure. The residue was treated with  
47 10 mL of 95% TFA-CH<sub>2</sub>Cl<sub>2</sub> for 1 h. The solvent was removed under vacuum and toluene (2 × 10  
48 mL) was added and evaporated to get rid of residual TFA. The crude, foam like material was  
49  
50  
51  
52  
53  
54  
55  
56  
57  
58  
59  
60

1  
2  
3 treated with Boc-Tle-OH (1.2 equiv), HBTU (1.2 equiv) and DIEA (3.0 equiv) for 12 h in dry  
4  
5 CH<sub>2</sub>Cl<sub>2</sub> (50 mL). The solvent was evaporated in vacuo and the residue was dissolved in EtOAc  
6  
7 and washed with 5% HCl (3 × 30 mL), 10% NaHCO<sub>3</sub> (2 × 30 mL) and brine. After drying  
8  
9 (MgSO<sub>4</sub>), filtration, and evaporation the residue was treated with 95%TFA-DCM for 1h. The  
10  
11 solvent was concentrated under vacuum and then diluted with water and neutralized the aqueous  
12  
13 solution with NH<sub>4</sub>OH and lyophilized to give an off-white foam. The amine was then treated  
14  
15 with **39b** (1.0 equiv) in 5 mL of dry NMP, NMM (3.0 equiv) and catalytic amount of DMAP  
16  
17 (0.05 equiv). After completion of the coupling, as monitored by HPLC, 25 mL of ether was  
18  
19 added to the reaction mixture and the resulting emulsion centrifuged. The clear supernatant was  
20  
21 decanted off and the crude precipitate was purified by HPLC using 0.1% TFA-MeCN/H<sub>2</sub>O.  
22  
23 Fractions containing pure phosphopeptide were combined and lyophilized to obtain pure  
24  
25 phosphopeptide/ phosphopeptidomimetic as a white powder. It was further dried over P<sub>2</sub>O<sub>5</sub>  
26  
27 chamber under vacuum at 37°C before used for affinity measurement. The yield, HRMS and  
28  
29 HPLC retention times are provided in the supporting information.  
30  
31  
32  
33  
34  
35

### 36 **Synthesis of $\beta$ MpCinn-Tle-Ala-NMe(Ph) (22) and $\beta$ MpCinn-Tle-(Me)Ala-NMe(Ph) (23):**

37  
38 These syntheses followed the same procedure as described for **21** starting with Boc-Ala-OH and  
39  
40 Boc-N(Me)Ala-OH respectively. Yields, HRMS and HPLC retention times are provided in the  
41  
42 supporting information.  
43  
44  
45

46 **Fluorescence Polarization Assays.** Peptides (200 $\mu$ M) in “fluorescence polarization buffer”  
47  
48 (FPB, 50 mM NaCl, 10 mM Hepes, 1 mM Na<sub>4</sub>EDTA, 2 mM DTT, and 1% NP-40 ) were placed  
49  
50 in 96 well plates and serial dilutions were carried out in the same buffer on a Biomek 2000 liquid  
51  
52 handling robot. Aliquots (50  $\mu$ L) of a solution of STAT6 (480 nM) and 20 nM of FAM-Ala-  
53  
54 pTyr-Lys-Pro-Phe-Gln-Asp-Leu-Ile-NH<sub>2</sub> in the same buffer were placed in wells of a second 96-  
55  
56 well plate using the robot. To each well of the second plate was added 50  $\mu$ L of the peptide  
57  
58  
59  
60

1  
2  
3 solutions from the first plate. Fluorescence polarization was then read on a Tecan Infinite  
4 F200Pro plate reader. With use of Prizm 6, from GraphPad Software, Inc., the mP was plotted  
5  
6 against the log of the peptide concentration and IC<sub>50</sub> values were obtained from non-linear  
7  
8 regression analysis. Peptides were assayed in triplicate using three separate STAT6-probe  
9  
10 preparations. IC<sub>50</sub> values are reported as the mean of three IC<sub>50</sub> values ± standard deviation.  
11  
12  
13

14 **Inhibition of Stat6 Tyrosine641 Phosphorylation in Intact Cells.** Beas-2B cells were seeded  
15  
16 on 6-well plates at a density of  $3.0 \times 10^5$  cells/well the day before treatment. Powdered prodrugs  
17  
18 were dissolved in DMSO to obtain 5-10 μM stock solutions. Aliquots of the stocks were added  
19  
20 to the cell cultures to reach the desired final concentrations of the prodrugs. Cultures were  
21  
22 incubated with prodrugs for 2 h and stimulated with IL-4 or IL-13 (2 ng/mL) for 1 h. Cells were  
23  
24 harvested, washed with ice-cold phosphate buffer saline (PBS) and lysed with cell lysis buffer  
25  
26 (Cell Signaling, #9803) supplemented with phenylmethanesulfonylfluoride (PMSF) serine  
27  
28 protease inhibitor. After incubation on ice for 10 min, cells were collected by scraping the dishes,  
29  
30 and the resulting suspensions were centrifuged at 13,200 rpm for 15 min at 4°C. The  
31  
32 supernatants were transferred to clean tubes, and aliquots (5 μL) were used to measure the  
33  
34 concentration of proteins using the modified Lowry protein assay (BioRad) on a Tecan Infinite  
35  
36 Pro 200 plate reader. Levels of pSTAT6 and total STAT6 proteins were estimated by western  
37  
38 blotting. Quantification of western blotting band density was performed using ImageJ software.  
39  
40  
41  
42  
43  
44  
45

46 **Western Blotting.** Aliquots of the whole cell lysate (15-30 μg proteins) were separated on a  
47  
48 10% SDS-PAGE polyacrylamide gel and transferred to PVDF membranes. The membranes were  
49  
50 blocked with a 3% BSA solution in TBST (1X tris-buffered saline, 0.1 % Tween 20) and probed  
51  
52 with phospho-Stat6(Tyr641) antibody (Cell Signaling, #9361) followed by incubation with  
53  
54 horseradish peroxidase conjugated secondary antibody (BioRad). Levels of pStat6 protein were  
55  
56 detected with ECL detection reagents (GE Healthcare Life Science) capturing the resulting  
57  
58  
59  
60

1  
2  
3 chemiluminescence signal on x-ray films. PVDF filters were then stripped with stripping buffer  
4  
5 at rt for 30 min, blocked with 3% BSA and probed with Stat6 antibody (Cell Signaling, #9362 or  
6  
7 Santa Cruz, sc-374021) whose signal was detected as described above.  
8  
9

10 **Effect of prodrugs on Beas-2B cell proliferation.** Effects of prodrugs on cell proliferation  
11  
12 were determined by MTS assay. Beas-2B cells were seeded on a 96-well plate (2000 cells/well).  
13  
14 Compounds were dissolved in DMSO to make 10 mM stock solutions. Stocks were subjected to  
15  
16 serial dilution in DMSO and equal amounts of each dilution were added to the cultures. After  
17  
18 incubation at 37 °C for 72 h, the culture medium was removed and a 1:5 MTS/PBS solution was  
19  
20 added to each well. The dish was then incubated for an additional 1 h and viable cells were  
21  
22 estimated by measuring the optical density of the samples at 490 nm.  
23  
24  
25  
26  
27  
28

29 **RT-PCR** RNA isolated from Beas-2B cells culture by Trizol (15596-026; Invitrogen, Grand  
30  
31 Island, NY) was subjected to cDNA synthesis with TaqMan Reverse Transcription kit  
32  
33 (N8080234; Applied Biosystems, Foster City, CA). Probes for CCL26 and  $\beta$ -actin were  
34  
35 purchased from Applied Biosystems (Foster City, CA) to quantify relative expression using  
36  
37 TaqMan Fast Universal PCR Master Mix (435189, Applied Biosystems, Foster City, CA) on a  
38  
39 the 7500 Real-Time PCR System (Applied Biosystems, Foster City, CA).  
40  
41  
42

43 **Mice.** C57BL/6J mice were purchased from Jackson Laboratories. Mice were housed in the SPF  
44  
45 animal facility at M.D. Anderson Cancer Center and all animal experiments were approved by  
46  
47 Institutional Animal Care and Use Committee.  
48  
49  
50

51  
52 **CD4<sup>+</sup> T cells activation and Immunoblot analysis.** CD4<sup>+</sup> T cells from C57BL/6J mice were  
53  
54 sorted by AutoMACS (Miltenyi Biotec) and activated with plate-bound anti-CD3 and/or anti-  
55  
56 CD28 (eBioscience) alone or together with IL2, IL-6 or IL-4 (Peprotech) for 15 minutes. Cells  
57  
58  
59  
60

1  
2  
3 were lysed in kinase assay lysis buffer supplemented with protease inhibitor cocktail (Roche)  
4  
5 and phosphatase inhibitors (10 mM NaF and 1 mM Na<sub>3</sub>VO<sub>4</sub>). Protein concentration was  
6  
7 determined by Bio-Rad Bradford protein assay and equal amounts of protein were loaded for  
8  
9 immunoblot analysis with antibodies against phospho-STAT1 (Tyr701), phospho-STAT3  
10  
11 (Ser727), phospho-STAT5 (Tyr694), phospho-STAT6 (Tyr641), STAT1, STAT3 (Cell  
12  
13 Signaling), STAT5 and STAT6 (Santa Cruz Biotechnology). Anti-mouse IgG-HRP, and anti-  
14  
15 rabbit IgG-HRP secondary antibodies were from Thermo scientific.  
16  
17  
18  
19  
20  
21

## 22 **Molecular Modeling**

23  
24 A homology model of STAT6 was obtained from ModBase, a database of comparative protein  
25  
26 structure models.<sup>37</sup> The homology model is based on the template structure of STAT1 (PDB ID  
27  
28 1YVL, chain A) and residues 445-631, comprising the SH2 domain and part of the linker domain  
29  
30 were used. Using DINC,<sup>35,36</sup> **18a** was docked to the SH2 domain of STAT6. The docked  
31  
32 structure was simulated in explicit water using a molecular dynamics program in AMBER  
33  
34 (version 11). Potentials for STAT6 were assigned with AMBER's ff99SB force field and those  
35  
36 of **18a** were assigned with GAFF force field. Point charges for **18a** were calculated using AM1-  
37  
38 BCC charge model. The solvated complex was minimized in three rounds with each round  
39  
40 involving 1000 steps (10 steps of steepest descent minimization followed by 990 steps of  
41  
42 conjugate gradient minimization). The solute (SH2 domain of STAT6) was restrained/fixd in  
43  
44 each round. The restraint weight was set to 5.0, 2.0, and 0.05 (kcal/mol-Å<sup>2</sup>) in rounds 1, 2, and 3,  
45  
46 respectively. The molecular dynamics protocol involved a temperature (300 K) equilibration step  
47  
48 for 100 ps, a pressure equilibration step for 400 ps, followed by a production run of 20 ns at  
49  
50 constant temperature and pressure. The time step used for the simulation was 2 fs and the  
51  
52 molecular dynamics trajectory was recorded every 1 ps. The structures of the complex derived  
53  
54  
55  
56  
57  
58  
59  
60

1  
2  
3 from the last 10 ns of the trajectory were clustered using k-means (k=5) clustering method and  
4  
5 the representative structure from the largest cluster was output as the model of **18a** in complex  
6  
7 with the STAT6 shown in Figure 3.  
8  
9

### 10 **Supporting Information**

11  
12 Yields and characterization of phosphopeptide inhibitors, phosphate analogs of **17**, and prodrug  
13  
14 analogs of **17**. Figures of the inhibition of pSTAT6 and pAkt in MDA-MB-468 breast cancer  
15  
16 cells and STAT proteins in CD4<sup>+</sup> T lymphocytes. NMR Characterization of **19c** and **31**.  
17  
18  
19 SMILES CSV file of compounds **1 - 55**.  
20  
21  
22  
23

### 24 **Author Information**

25  
26  
27 E mail: \* [jmcmurra@mdanderson.org](mailto:jmcmurra@mdanderson.org) Telephone: 713-745-3763. Fax: 713-745-1710  
28

### 29 **Notes**

30  
31  
32 The authors declare no competing financial interest  
33  
34  
35

36  
37 **Acknowledgements.** We are grateful to the American Asthma Foundation (Award Number: 11-  
38  
39 0360), the Keck Center Computational Cancer Biology Training Program of the Gulf Coast  
40  
41 Consortia (CPRIT RP101489) and the National Science Foundation (ABI 0960612 at Rice  
42  
43 University) for support of this work. We are also grateful to the MDACC Institutional Research  
44  
45 Grant and the CTT/TI-3D Chemistry & Molecularly Targeted Therapeutic Development Grant  
46  
47 Program. We also acknowledge the Cancer Center Support Grant P30 CA016672 at MDACC  
48  
49 for support of both the NMR facility and the Translational Chemistry Core Facility (mass  
50  
51 spectrometry). Beas-2B cells were a kind gift from Walter Hittleman.  
52  
53  
54  
55  
56  
57  
58  
59  
60

**Abbreviations:** DIEA, diisopropylethylamine; DIPCDI, diisopropylcarbodiimide; Fmoc, 9-fluorenylmethoxycarbonyl; HBTU, *O*-(Benzotriazol-1-yl)-*N,N,N,N*-tetramethyluronium hexafluorophosphate; HOBt, 1-hydroxybenzotriazole; IL-4, interleukin 4; IL-13, interleukin 13; JAK, Janus kinase; pCinn, 4-phosphoryloxy cinnamide;  $\beta$ MpCinn,  $\beta$ -methyl pCinn or [2*E*] 3-(4-phosphoryloxyphenyl)-2-butenamide;  $\beta$ MF2PmCinn, [2*E*] 3-[4-[(phosphinyl)difluoromethyl]phenyl]-2-butenamide; POM, pivaloyloxymethyl; SAR, structure activity relationship; SH2 domain, Src homology 2 domain; STAT3, signal transducer and activator of transcription 3; STAT6, signal transducer and activator of transcription 6; TES, triethylsilane; Th2, Helper T cell type 2; TIS, triisopropylsilane.

## References

1. Kuperman, D. A.; Schleimer, R. P. Interleukin-4, interleukin-13, signal transducer and activator of transcription factor 6, and allergic asthma. *Curr. Mol. Med.* **2008**, *8*, 384-392.
2. Oh, C. K.; Geba, G. P.; Molino, N. Investigational therapeutics targeting the IL-4/IL-13/STAT-6 pathway for the treatment of asthma. *Eur. Respir. Rev.* **2010**, *19*, 46-54.
3. Walford, H. H.; Doherty, T. A. STAT6 and lung inflammation. *JAK-STAT* **2013**, *2*, e25301.
4. Biswas, S. K.; Chittezhath, M.; Shalova, I. N.; Lim, J. Y. Macrophage polarization and plasticity in health and disease. *Immunol. Res.* **2012**, *53*, 11-24.
5. Mullings, R. E.; Wilson, S. J.; Puddicombe, S. M.; Lordan, J. L.; Bucchieri, F.; Djukanovic, R.; Howarth, P. H.; Harper, S.; Holgate, S. T.; Davies, D. E. Signal transducer and activator of transcription 6 (STAT-6) expression and function in asthmatic bronchial epithelium. *J. Allergy Clin. Immunol.* **2001**, *108*, 832-838.

- 1  
2  
3  
4  
5  
6  
7  
8  
9  
10  
11  
12  
13  
14  
15  
16  
17  
18  
19  
20  
21  
22  
23  
24  
25  
26  
27  
28  
29  
30  
31  
32  
33  
34  
35  
36  
37  
38  
39  
40  
41  
42  
43  
44  
45  
46  
47  
48  
49  
50  
51  
52  
53  
54  
55  
56  
57  
58  
59  
60
6. Darcan-Nicolaisen, Y.; Meinicke, H.; Fels, G.; Hegend, O.; Haberland, A.; Kuhl, A.; Loddenkemper, C.; Witzentrath, M.; Kube, S.; Henke, W.; Hamelmann, E. Small interfering RNA against transcription factor STAT6 inhibits allergic airway inflammation and hyperreactivity in mice. *J. Immunol.* **2009**, *182*, 7501-7508.
7. Chiba, Y.; Todoroki, M.; Nishida, Y.; Tanabe, M.; Misawa, M. A novel STAT6 inhibitor AS1517499 ameliorates antigen-induced bronchial hypercontractility in mice. *Am. J. Respir. Cell Mol. Biol.* **2009**, *41*, 516-524.
8. Nagashima, S.; Hondo, T.; Nagata, H.; Ogiyama, T.; Maeda, J.; Hoshii, H.; Kontani, T.; Kuromitsu, S.; Ohga, K.; Orita, M.; Ohno, K.; Moritomo, A.; Shiozuka, K.; Furutani, M.; Takeuchi, M.; Ohta, M.; Tsukamoto, S. Novel 7H-pyrrolo[2,3-d]pyrimidine derivatives as potent and orally active STAT6 inhibitors. *Bioorg. Med. Chem.* **2009**, *17*, 6926-6936.
9. Nagashima, S.; Nagata, H.; Iwata, M.; Yokota, M.; Moritomo, H.; Orita, M.; Kuromitsu, S.; Koakutsu, A.; Ohga, K.; Takeuchi, M.; Ohta, M.; Tsukamoto, S. Identification of 4-benzylamino-2-[(4-morpholin-4-ylphenyl)amino]pyrimidine-5-carboxamide derivatives as potent and orally bioavailable STAT6 inhibitors. *Bioorg. Med. Chem.* **2008**, *16*, 6509-6521.
10. Nagashima, S.; Yokota, M.; Nakai, E.; Kuromitsu, S.; Ohga, K.; Takeuchi, M.; Tsukamoto, S.; Ohta, M. Synthesis and evaluation of 2-[[2-(4-hydroxyphenyl)-ethyl]amino]pyrimidine-5-carboxamide derivatives as novel STAT6 inhibitors. *Bioorg. Med. Chem.* **2007**, *15*, 1044-1055.
11. Ohga, K.; Kuromitsu, S.; Takezawa, R.; Numazaki, M.; Ishikawa, J.; Nagashima, S.; Shimizu, Y. YM-341619 suppresses the differentiation of spleen T cells into Th2 cells in vitro, eosinophilia, and airway hyperresponsiveness in rat allergic models. *Eur. J. Pharmacol.* **2008**, *590*, 409-416.

- 1  
2  
3  
4  
5  
6  
7  
8  
9  
10  
11  
12  
13  
14  
15  
16  
17  
18  
19  
20  
21  
22  
23  
24  
25  
26  
27  
28  
29  
30  
31  
32  
33  
34  
35  
36  
37  
38  
39  
40  
41  
42  
43  
44  
45  
46  
47  
48  
49  
50  
51  
52  
53  
54  
55  
56  
57  
58  
59  
60
12. Tanabe, T.; Kanoh, S.; Tsushima, K.; Yamazaki, Y.; Kubo, K.; Rubin, B. K. Clarithromycin inhibits interleukin-13-induced goblet cell hyperplasia in human airway cells. *Am. J. Respir. Cell Mol. Biol.* **2011**, *45*, 1075-1083.
13. Zhou, L.; Kawate, T.; Liu, X.; Kim, Y. B.; Zhao, Y.; Feng, G.; Banerji, J.; Nash, H.; Whitehurst, C.; Jindal, S.; Siddiqui, A.; Seed, B.; Wolfe, J. L. STAT6 phosphorylation inhibitors block eotaxin-3 secretion in bronchial epithelial cells. *Bioorg. Med. Chem.* **2012**, *20*, 750-758.
14. Kudlacz, E.; Conklyn, M.; Andresen, C.; Whitney-Pickett, C.; Changelian, P. The JAK-3 inhibitor CP-690550 is a potent anti-inflammatory agent in a murine model of pulmonary eosinophilia. *Eur. J. Pharmacol.* **2008**, *582*, 154-161.
15. Matsunaga, Y.; Inoue, H.; Fukuyama, S.; Yoshida, H.; Moriwaki, A.; Matsumoto, T.; Matsumoto, K.; Asai, Y.; Kubo, M.; Yoshimura, A.; Nakanishi, Y. Effects of a Janus kinase inhibitor, pyridone 6, on airway responses in a murine model of asthma. *Biochem. Biophys. Res. Commun.* **2011**, *404*, 261-267.
16. Wang, L. H.; Yang, X. Y.; Kirken, R. A.; Resau, J. H.; Farrar, W. L. Targeted disruption of stat6 DNA binding activity by an oligonucleotide decoy blocks IL-4-driven T(H)2 cell response. *Blood* **2000**, *95*, 1249-1257.
17. McCusker, C. T.; Wang, Y.; Shan, J.; Kinyanjui, M. W.; Villeneuve, A.; Michael, H.; Fixman, E. D. Inhibition of experimental allergic airways disease by local application of a cell-penetrating dominant-negative STAT-6 peptide. *J. Immunol.* **2007**, *179*, 2556-2564.
18. Stolzenberger, S.; Haake, M.; Duschl, A. Specific inhibition of interleukin-4-dependent Stat6 activation by an intracellularly delivered peptide. *Eur. J. Biochem.* **2001**, *268*, 4809-4814.
19. Wang, Y.; Li, Y.; Shan, J.; Fixman, E.; McCusker, C. Effective treatment of experimental ragweed-induced asthma with STAT-6-IP, a topically delivered cell-penetrating peptide. *Clin. Exp. Allergy* **2011**, *41*, 1622-1630.

- 1  
2  
3 20. Blease, K. Therapeutics targeting IL-13 for the treatment of pulmonary inflammation and  
4  
5 airway remodeling. *Curr. Opin. Investig. Drugs* **2008**, *9*, 1180-1184.  
6  
7  
8 21. Walsh, G. M. An update on emerging drugs for asthma. *Expert Opin. Emerg. Drugs*  
9  
10 **2012**, *17*, 37-42.  
11  
12 22. Wenzel, S.; Ford, L.; Pearlman, D.; Spector, S.; Sher, L.; Skobieranda, F.; Wang, L.;  
13  
14 Kirkesseli, S.; Rocklin, R.; Bock, B.; Hamilton, J.; Ming, J. E.; Radin, A.; Stahl, N.;  
15  
16 Yancopoulos, G. D.; Graham, N.; Pirozzi, G. Dupilumab in persistent asthma with elevated  
17  
18 eosinophil levels. *N Engl J Med* **2013**, *368*, 2455-2466.  
19  
20  
21 23. McKinney, J.; Raimundo, B. C.; Cushing, T. D.; Yoshimura, H.; Ohuchi, Y.; Hiratate,  
22  
23 A.; Fukushima, H. Preparation of peptides as inhibitors of STAT function. US 6426331 B1,  
24  
25 2002.  
26  
27  
28 24. McKinney, J.; Raimundo, B. C.; Cushing, T. D.; Yoshimura, H.; Ohuchi, Y.; Hiratate,  
29  
30 A.; Fukushima, H.; Xu, F.; Peto, C. STAT4 and STAT6 binding dipeptide derivatives. WO  
31  
32 2001083517 20000503., 2001.  
33  
34  
35 25. Songyang, Z.; Shoelson, S. E.; Chaudhuri, M.; Gish, G.; Pawson, T.; Haser, W. G.; King,  
36  
37 F.; Roberts, T.; Ratnofsky, S.; Lechleider, R. J.; Neel, B. G.; B., B. R.; Fajardof, J. E.; Chouf, M.  
38  
39 M.; Hanafusa, H.; Schaffhausen, B.; Cantley, L. C. SH2 domains recognize specific  
40  
41 phosphopeptide sequences. *Cell* **1993**, *72*, 767-778.  
42  
43  
44 26. Songyang, Z.; Shoelson, S. E.; McGlade, J.; Olivier, P.; Pawson, T.; Bustelo, X. R.;  
45  
46 Barbacid, M.; Sabe, H.; Hanafusa, H.; Yi, T.; Ren, R.; Baltimore, D.; Ratnofsky, S.; Feldman, R.  
47  
48 A.; Cantley, L. C. Specific motifs recognized by the SH2 domains of Csk, 3BP2, fps/fes, GRB-2,  
49  
50 HCP, SHC, Syk, and Vav. *Mol. Cell. Biol.* **1994**, *14*, 2777-2785.  
51  
52  
53 27. Wu, P.; Brasseur, M.; Schindler, U. A high-throughput STAT binding assay using  
54  
55 fluorescence polarization. *Anal. Biochem.* **1997**, *249*, 29-36.  
56  
57  
58  
59  
60

- 1  
2  
3 28. Mandal, P. K.; Limbrick, D.; Coleman, D. R.; Dyer, G. A.; Ren, Z.; Birtwistle, J. S.;  
4 Xiong, C.; Chen, X.; Briggs, J. M.; McMurray, J. S. Conformationally constrained  
5  
6 peptidomimetic inhibitors of signal transducer and activator of transcription 3: evaluation and  
7  
8 molecular modeling. *J. Med. Chem.* **2009**, *52*, 2429-2442.  
9  
10  
11  
12 29. Burke, T. R., Jr.; Smyth, M. S.; Otaka, A.; Nomizu, M.; Roller, P. P.; Wolf, G.; Case, R.;  
13  
14 Shoelson, S. E. Nonhydrolyzable phosphotyrosyl mimetics for the preparation of phosphatase-  
15  
16 resistant SH2 domain inhibitors. *Biochemistry* **1994**, *33*, 6490-6494.  
17  
18  
19  
20 30. Farquhar, D.; Khan, S.; Srivastva, D. N.; Saunders, P. P. Synthesis and antitumor  
21  
22 evaluation of bis[(pivaloyloxy)methyl] 2'-deoxy-5-fluorouridine 5'-monophosphate (FdUMP): a  
23  
24 strategy to introduce nucleotides into cells. *J. Med. Chem.* **1994**, *37*, 3902-3909.  
25  
26  
27 31. Mandal, P. K.; Gao, F.; Lu, Z.; Ren, Z.; Ramesh, R.; Birtwistle, J. S.; Kaluarachchi, K.  
28  
29 K.; Chen, X.; Bast, R. C.; Liao, W. S.; McMurray, J. S. Potent and selective phosphopeptide  
30  
31 mimetic prodrugs targeted to the Src homology 2 (SH2) domain of signal transducer and  
32  
33 activator of transcription 3. *J. Med. Chem.* **2011**, *54*, 3549-5463.  
34  
35  
36 32. Mandal, P. K.; Liao, W. S.; McMurray, J. S. Synthesis of phosphatase-stable, cell-  
37  
38 permeable peptidomimetic prodrugs that target the SH2 domain of Stat3. *Org. Lett.* **2009**, *11*,  
39  
40 3394-3397.  
41  
42  
43 33. Morlacchi, P.; Mandal, P. K.; McMurray, J. S. Synthesis and in vitro evaluation of a  
44  
45 peptidomimetic inhibitor targeting the Src homology 2 (SH2) domain of STAT6. *ACS Med.*  
46  
47 *Chem. Lett.* **2014**, *5*, 69-72.  
48  
49  
50 34. Coleman, D. R. I. V.; Kaluarachchi, K.; Ren, Z.; Chen, X.; McMurray, J. S. Solid phase  
51  
52 synthesis of phosphopeptides incorporating 2,2-dimethyloxazolidine pseudoproline analogs:  
53  
54 evidence for trans Leu-Pro peptide bonds in Stat3 inhibitors. *Int. J. Pept. Res. Ther.* **2008**, *14*, 1-  
55  
56  
57  
58  
59  
60 9.

- 1  
2  
3 35. Dhanik, A.; McMurray, J. S.; Kaviraki, L. E. DINC: a new AutoDock-based protocol for  
4 docking large ligands. *BMC Struct Biol* **2013**, *13 Suppl 1*, S11.  
5  
6  
7  
8 36. Dhanik, A.; McMurray, J. S.; Kaviraki, L. E. Binding modes of peptidomimetics designed  
9 to inhibit STAT3. *PLoS One* **2012**, *7*, e51603.  
10  
11  
12 37. Pieper, U.; Webb, B. M.; Barkan, D. T.; Schneidman-Duhovny, D.; Schlessinger, A.;  
13 Braberg, H.; Yang, Z.; Meng, E. C.; Pettersen, E. F.; Huang, C. C.; Datta, R. S.; Sampathkumar,  
14 P.; Madhusudhan, M. S.; Sjoelander, K.; Ferrin, T. E.; Burley, S. K.; Sali, A. ModBase, a  
15 database of annotated comparative protein structure models, and associated resources. *Nucleic  
16 Acids Res.* **2011**, *39*, D465-D474.  
17  
18  
19  
20 38. Chen, X.; Vinkemeier, U.; Zhao, Y.; Jeruzalmi, D.; Darnell, J. E., Jr.; Kuriyan, J. Crystal  
21 structure of a tyrosine phosphorylated STAT-1 dimer bound to DNA. *Cell* **1998**, *93*, 827-839.  
22  
23  
24 39. Mao, X.; Ren, Z.; Parker, G. N.; Sondermann, H.; Pastorello, M. A.; Wang, W.;  
25 McMurray, J. S.; Demeler, B.; Darnell, J. E., Jr.; Chen, X. Structural bases of unphosphorylated  
26 STAT1 association and receptor binding. *Mol. Cell* **2005**, *17*, 761-771.  
27  
28  
29 40. Becker, S.; Groner, B.; Muller, C. W. Three-dimensional structure of the Stat3beta  
30 homodimer bound to DNA. *Nature* **1998**, *394*, 145-151.  
31  
32  
33 41. McMurray, J. S. Structural basis for the binding of high affinity phosphopeptides to  
34 Stat3. *Biopolymers* **2008**, *90*, 69-79.  
35  
36  
37 42. Mandal, P. K.; Ren, Z.; Chen, X.; Kaluarachchi, K.; Liao, W. S. L.; McMurray, J. S.  
38 Structure-activity studies of phosphopeptidomimetic prodrugs targeting the Src homology 2  
39 (SH2) domain of signal transducer and activator of transcription 3 (Stat3). *Int. J. Pept. Res. Ther.*  
40 **2013**, *19*, 3-12.  
41  
42  
43  
44  
45  
46 43. Lu, Y.; Lin, Y. Z.; LaPushin, R.; Cuevas, B.; Fang, X.; Yu, S. X.; Davies, M. A.; Khan,  
47 H.; Furui, T.; Mao, M.; Zinner, R.; Hung, M. C.; Steck, P.; Siminovitch, K.; Mills, G. B. The  
48  
49  
50  
51  
52  
53  
54  
55  
56  
57  
58  
59  
60

1  
2  
3 PTEN/MMAC1/TEP tumor suppressor gene decreases cell growth and induces apoptosis and  
4 anoikis in breast cancer cells. *Oncogene* **1999**, *18*, 7034-7045.

5  
6  
7  
8 44. Workman, P. Inhibiting the phosphoinositide 3-kinase pathway for cancer treatment.  
9  
10 *Biochem Soc Trans* **2004**, *32*, 393-396.

11  
12 45. Hoeck, J.; Woisetschlager, M. Activation of eotaxin-3/CCL126 gene expression in human  
13 dermal fibroblasts is mediated by STAT6. *J Immunol* **2001**, *167*, 3216-3222.

14  
15  
16  
17 46. Hoshino, A.; Tsuji, T.; Matsuzaki, J.; Jinushi, T.; Ashino, S.; Teramura, T.; Chamoto, K.;  
18 Tanaka, Y.; Asakura, Y.; Sakurai, T.; Mita, Y.; Takaoka, A.; Nakaike, S.; Takeshima, T.; Ikeda,  
19 H.; Nishimura, T. STAT6-mediated signaling in Th2-dependent allergic asthma: critical role for  
20 the development of eosinophilia, airway hyper-responsiveness and mucus hypersecretion,  
21 distinct from its role in Th2 differentiation. *Int Immunol* **2004**, *16*, 1497-1505.

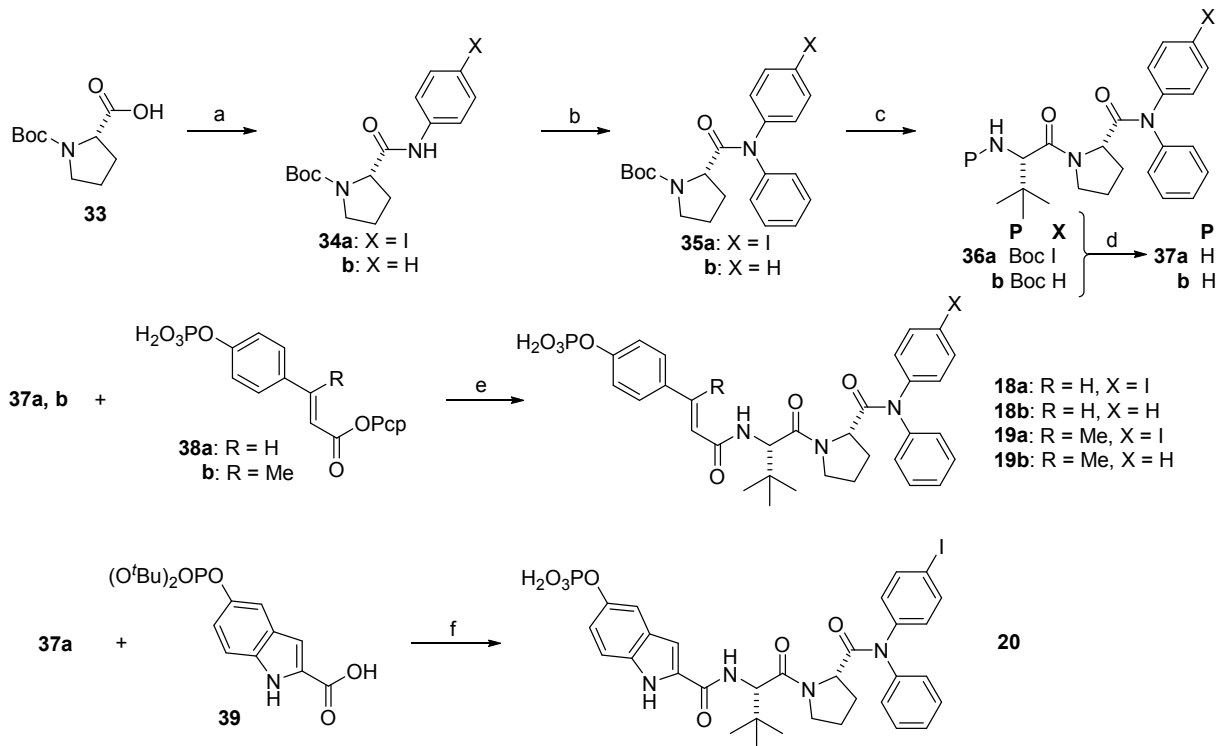
22  
23  
24  
25 47. Chao, H.-G.; Leiting, B.; Reiss, P. D.; Burkhardt, A. L.; Klimas, C. E.; Bolen, J. B.;  
26 Matsueda, G. R. Synthesis and application of Fmoc-O-[bis(dimethylamino)phosphono]tyrosine,  
27 a versatile protected phosphotyrosine equivalent. *J. Org. Chem.* **1995**, *60*, 7710-7711.

28  
29  
30  
31 48. Ueki, M.; Goto, M.; Okumura, J.; Ishii, Y. N,N'-dialkyldiamide-type phosphate  
32 protecting groups for Fmoc synthesis of phosphotyrosine-containing peptides: optimization of  
33 the alkyl group. *Bull. Chem. Soc. Jpn.* **1998**, *71*, 1887-1898.

34  
35  
36  
37 49. Ueki, M.; Tachibana, J.; Ishii, Y.; Okumura, J.; Goto, M. N,N'-Dialkyldiamide-type  
38 phosphate protecting groups for Fmoc synthesis of phosphotyrosine-containing peptides.  
39  
40  
41  
42 *Tetrahedron Lett.* **1996**, *37*, 4953-4956.

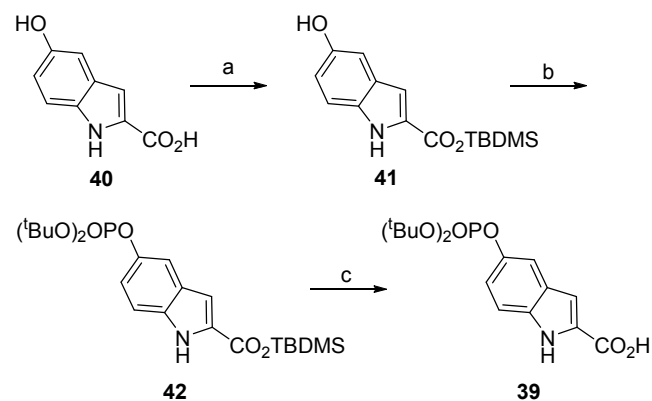
43  
44  
45  
46 50. Pearson, D. A.; Blanchette, M.; Baker, M. L.; Guindon, C. A. Trialkylsilanes as  
47 scavengers for the trifluoroacetic acid deblocking of protecting groups in peptide synthesis.  
48  
49  
50  
51  
52  
53  
54  
55  
56  
57  
58  
59  
60 *Tetrahedron Letters* **1989**, *30*, 2739-2742.

- 1  
2  
3  
4  
5  
6  
7  
8  
9  
10  
11  
12  
13  
14  
15  
16  
17  
18  
19  
20  
21  
22  
23  
24  
25  
26  
27  
28  
29  
30  
31  
32  
33  
34  
35  
36  
37  
38  
39  
40  
41  
42  
43  
44  
45  
46  
47  
48  
49  
50  
51  
52  
53  
54  
55  
56  
57  
58  
59  
60
51. Barton, D. H. R.; Finet, J. P.; Khamsi, J. Copper salt catalysis of N-phenylation of amines by trivalent organobismuth compounds. *Tetrahedron Lett.* **1987**, *28*, 887-890.
52. Chan, D. M. T. Promotion of reaction of N-H bonds with triarylbismuth and cupric acetate. *Tetrahedron Lett.* **1996**, *37*, 9013-9016.
53. Coleman, D. R. t.; Ren, Z.; Mandal, P. K.; Cameron, A. G.; Dyer, G. A.; Muranjan, S.; Campbell, M.; Chen, X.; McMurray, J. S. Investigation of the binding determinants of phosphopeptides targeted to the SRC homology 2 domain of the signal transducer and activator of transcription 3. Development of a high-affinity peptide inhibitor. *J. Med. Chem.* **2005**, *48*, 6661-6670.
54. Ren, Z.; Cabell, L. A.; Schaefer, T. S.; McMurray, J. S. Identification of a high-affinity phosphopeptide inhibitor of Stat3. *Bioorg. Med. Chem. Lett.* **2003**, *13*, 633-636.
55. Takatori, H.; Nakajima, H.; Hirose, K.; Kagami, S.; Tamachi, T.; Suto, A.; Suzuki, K.; Saito, Y.; Iwamoto, I. Indispensable role of Stat5a in Stat6-independent Th2 cell differentiation and allergic airway inflammation. *J Immunol* **2005**, *174*, 3734-3740.
56. Kawabata, T.; Matsuda, S.; Kawakami, S.; Monguchi, D.; Moriyama, K. Stereochemical diversity in asymmetric cyclization via memory of chirality. *J. Am. Chem. Soc.* **2006**, *128*, 15394-15395.

**Scheme 1.** Synthesis of bis-arylamide inhibitors of STAT6.

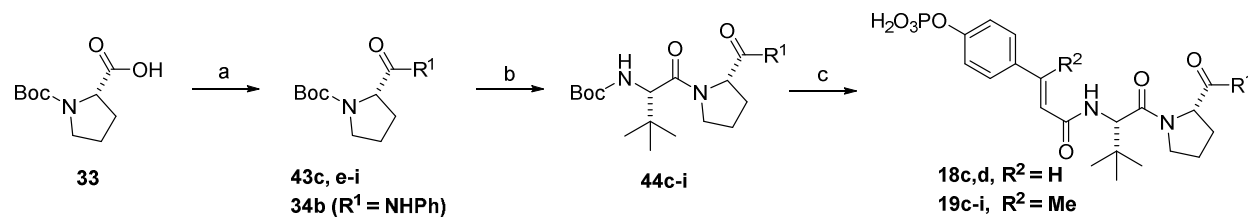
Reagents and Conditions: a) EDC, 4-iodoaniline (for **34a**) or aniline (for **34b**), DCM, rt 12h; b)  $\text{Ph}_3\text{Bi}$ ,  $\text{Cu}(\text{OAc})_2$ , TEA, DCM, 24h; c) i) neat TFA, ii) Boc-Tle-OH, HBTU, DIPEA, DCM rt 6h, d) neat TFA; e) NMP, NMM, DMAP (cat), rt, 3h, f) i) HBTU, DIPEA, DCM, 6h, ii) neat TFA, 1h.

**Scheme 2.** Synthesis of the phosphotyrosine mimic, 2-(di-*tert*-butylphosphoryloxy)indole-2-carboxylic acid.



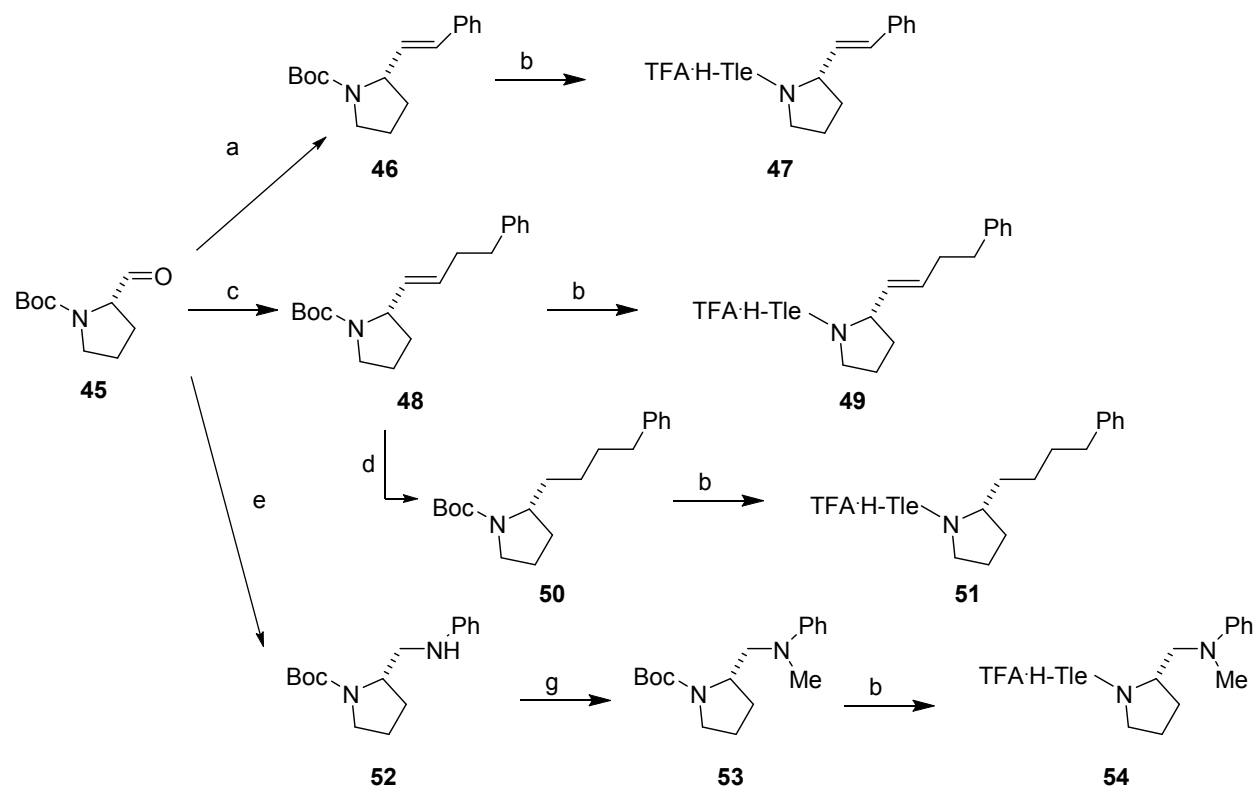
Reagents and Conditions: a) TBDMS-Cl, NMM; b) i, (tBuO)<sub>2</sub>PNEt<sub>2</sub>, 1*H*-Tetrazole, ii, tBuOOH; c) H<sub>3</sub>O<sup>+</sup>.

**Scheme 3.** Synthesis of C-terminal amide substitutions.



c, R<sub>1</sub> = N(Me)Ph; d, R<sub>1</sub> = NHPH; e R<sub>1</sub> = NHCH<sub>2</sub>Ph; f, R<sub>1</sub> = NHCH<sub>2</sub>CH<sub>2</sub>Ph; g, R<sub>1</sub> = N(Me)(C<sub>6</sub>H<sub>11</sub>); h R<sub>1</sub> = N(Me)<sub>2</sub>; i, R<sub>1</sub> = N(Et)<sub>2</sub>

Reagents and conditions: a) EDC, amine, DCM, rt, 12h; b) i) neat TFA; ii) HBTU, DIPEA, Boc-Tle-OH; iii) neat TFA; c) 38a or 38b, NMM, NMP, DMAP(cat).

**Scheme 4.** Synthesis of prolyl surrogates with amide bond replacements.

Reagents and conditions. a) NaH, PhCH<sub>2</sub>PPh<sub>3</sub>Br, THF; b) i) TFA; ii) Boc-Tle-OH, HBTU, DIPEA, iii) TFA; c) NaH, PhCH<sub>2</sub>CH<sub>2</sub>CH<sub>2</sub>PPh<sub>3</sub>Br, THF; d) H<sub>2</sub>, 10%Pd-C; e) Aniline, NaCNBH<sub>3</sub>, MeOH-AcOH; g) Formaldehyde (40% solution), NaCNBH<sub>3</sub>, MeOH-AcOH.

**Scheme 5.** Synthesis of prodrug analogs of **17**. See Chart 1 for structures.

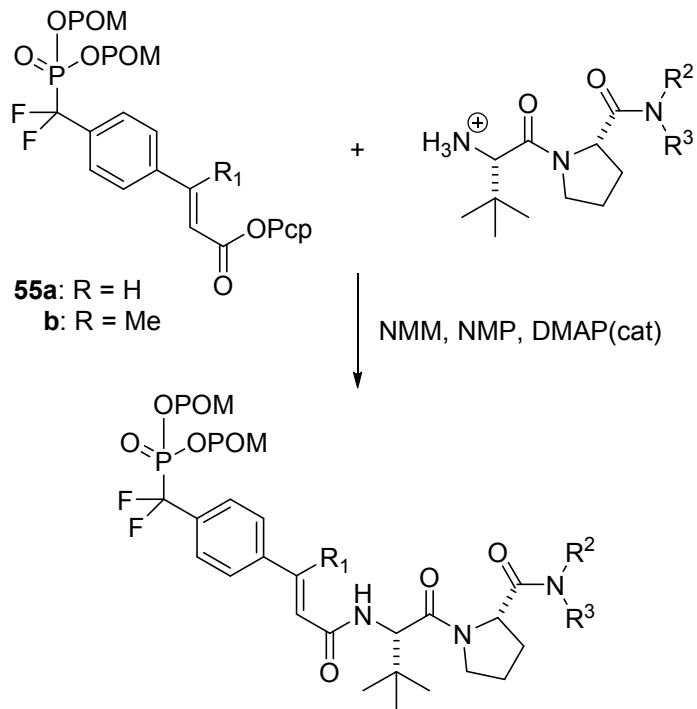


**Table 1:** Affinity of phosphopeptides based on Tyr631 of IL-4R $\alpha$  for STAT6.

	<b>Phosphopeptide</b>	<b>IC<sub>50</sub> (<math>\mu</math>M)</b>
<b>1</b>	Ac-pTyr-Lys-Pro-Phe-Gln-Asp-Leu-Ile-NH <sub>2</sub>	1.8 $\pm$ 0.27
<b>2</b>	Ac-pTyr-Lys-Pro-Phe-Gln-Asp-Leu-NH <sub>2</sub>	2.4 $\pm$ 0.66
<b>3</b>	Ac-pTyr-Lys-Pro-Phe-Gln-Asp-NH <sub>2</sub>	4.5 $\pm$ 0.033
<b>4</b>	Ac-pTyr-Lys-Pro-Phe-Gln-NH <sub>2</sub>	4.2 $\pm$ 0.25
<b>5</b>	Ac-pTyr-Lys-Pro-Phe-NH <sub>2</sub>	6.1 $\pm$ 1.2
<b>6</b>	Ac-pTyr-Lys-Pro-NH <sub>2</sub>	5.2 $\pm$ 0.096

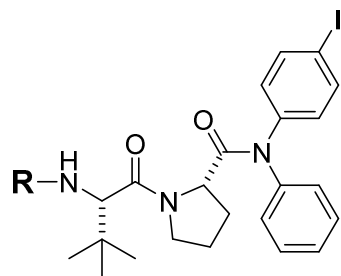
**Table 2:** *N*-Terminal derivatization and amino acid substitutions at position pY+1 in tetrapeptide **Xaa-pTyr-Ybb-Pro-Phe-NH<sub>2</sub>**

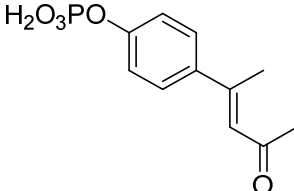
	<b>Xaa</b>	<b>Ybb</b>	<b>IC<sub>50</sub> (<math>\mu</math>M)</b>
<b>5</b>	CH <sub>3</sub> CO	Lys	6.1 $\pm$ 1.2
<b>7</b>	CH <sub>3</sub> CO	Tle	4.0 $\pm$ 1.2
<b>8</b>	CH <sub>3</sub> CO	Nle	5.2 $\pm$ 1.2
<b>9</b>	CH <sub>3</sub> CO	Ala	14.9 $\pm$ 1.6
<b>10</b>	PhCH <sub>2</sub> CH <sub>2</sub> CO	Lys	8.1 $\pm$ 2.7
<b>11</b>	PhCH <sub>2</sub> CO	Lys	4.1 $\pm$ 2.3
<b>12</b>	PhCO	Lys	3.5 $\pm$ 0.78
<b>13</b>	PhCH=CHCO	Lys	6.6 $\pm$ 0.37

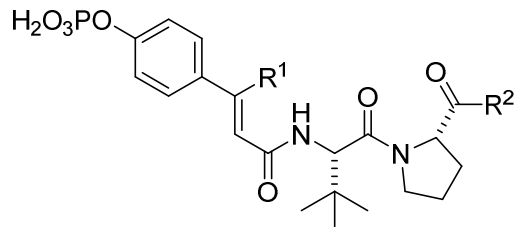
**Table 3.** Effect of constrained pTyr surrogates on the affinity of Xaa-Lys-Pro-Phe-NH<sub>2</sub>

Xaa	IC <sub>50</sub> (μM)
<b>5</b> Ac-pTyr	6.1 ± 1.2
<b>14</b> pCinn	8.6 ± 2.8
<b>15</b> p-Indole	3.7 ± 0.052
<b>16</b> p-Benzofuran	89.6 ± 1.5

**Table 4.** Effect of constrained pTyr surrogates on affinity for phosphodipeptide **R**-Tle-Pro-N(Ph)(4-I-Phe) for STAT6



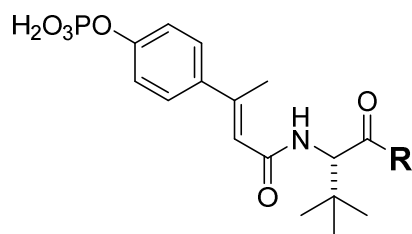
<b>R</b>	IC <sub>50</sub> (μM)
<b>18a</b> pCinn	0.044 ± 0.016
βMpCinn	
<b>19a</b> 	0.028 ± 0.006
<b>20</b> p-Indole	0.14 ± 0.06

**Table 5.** Effect of C-terminal substitution on affinity for STAT6

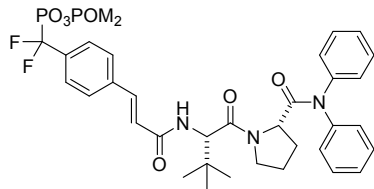
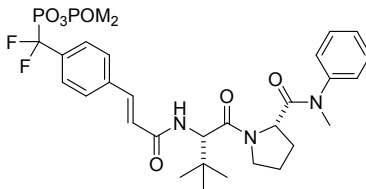
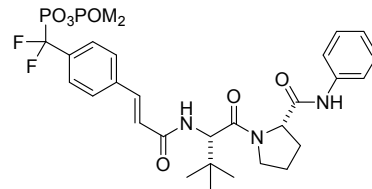
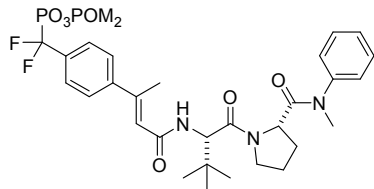
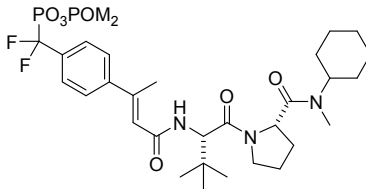
#	R <sup>1</sup>	R <sup>2</sup>	IC <sub>50</sub> (μM)
<b>18a</b>	H	NPh(4-I-Ph)	0.044 ± 0.016
<b>18b</b>	H	NPh <sub>2</sub>	0.120 ± 0.04
<b>18c</b>	H	N(Me)Ph	0.87 ± 0.03
<b>18d</b>	H	NHPh	1.25 ± 0.34
<b>19a</b>	Me	NPh(4-I-Ph)	0.028 ± 0.006
<b>19b</b>	Me	NPh <sub>2</sub>	0.089 ± 0.01
<b>19c</b>	Me	N(Me)Ph	0.12 ± 0.03
<b>19d</b>	Me	NHPh	0.27 ± 0.07
<b>19e</b>	Me	NHCH <sub>2</sub> Ph	0.34 ± 0.07
<b>19f</b>	Me	NHCH <sub>2</sub> CH <sub>2</sub> Ph	0.25 ± 0.06
<b>19g</b>	Me	N(Me)(C <sub>6</sub> H <sub>11</sub> )	0.23 ± 0.14
<b>19h</b>	Me	N(Me) <sub>2</sub>	0.74 ± 0.34
<b>19i</b>	Me	N(Et) <sub>2</sub>	0.38 ± 0.09

**Table 6.** Effect of proline replacements on  $\beta$ MpCinn-Tle-Xaa-N(Me)Ph

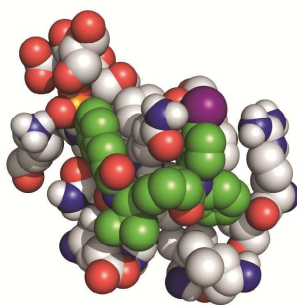
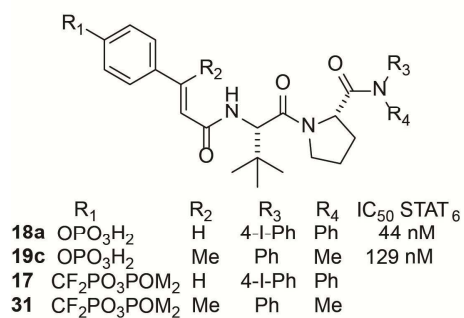
Xaa	IC <sub>50</sub> ( $\mu$ M)
<b>19c</b> Proline	0.12 $\pm$ 0.03
<b>21</b> Sarcosine	0.27 $\pm$ 0.05
<b>22</b> Alanine	0.12 $\pm$ 0.016
<b>23</b> <i>N</i> -Methyl-Alanine	0.48 $\pm$ 0.094

**Table 7.** Effect of modifications of the C-terminal amide bond.

#	R	IC <sub>50</sub> ( $\mu$ M)
<b>24</b>		3.43 $\pm$ 0.95
<b>25</b>		0.54 $\pm$ 0.11
<b>26</b>		1.07 $\pm$ 0.17
<b>27</b>		0.41 $\pm$ 0.05

**Chart 1.** Structures of prodrug analogs of **17****28****29****30****31****32**

## TOC Graphic

**18a**-STAT6 SH2 domain complex